CHAPTER 3
PLASTICS AND RUBBER

Richard E. Lyon
Fire Safety Branch AAR-440
Federal Aviation Administration
William J. Hughes Technical Center
Atlantic City International Airport, NJ 08405

3.1 INTRODUCTION

Plastics represent a large and growing fraction of the fire load in public and residential environments, yet relatively little is known about the factors that govern their fire behavior. This is due in large part to the variety of plastics in use, the large number of flammability tests, and the lack of a consensus opinion on what standardized fire test method(s) of fire response best describes the fire hazard. Moreover, the most widely used plastics are those that are least expensive and these tend to be the most flammable. Fig. 3.1 shows the fire hazard (see heat release capacity, Sec. 3.3) versus the truckload price of commercial plastics and elastomers. It is seen that fire hazard and cost span over two orders of magnitude, but the commodity and engineering plastics costing less than $10 per pound comprise over 95 percent of plastics in use and these vary by about a factor of 10 in flammability and price. Specialty plastics costing over $10 per pound are typically heat and chemical resistant (e.g., polymers with aromatic backbones and fluoroplastics) and these tend to also be of low flammability. This chapter examines passive fire protection from a materials engineering perspective. The goal is to develop an understanding of the relationship between the fire behavior of plastics and their properties and identify flammability parameters that can be measured, tabulated, and used to predict fire hazard. Several books have reviewed the flammability parameters of solids [1–17], liquids, and gases [18–20] in relation to their fire behavior.

3.2 POLYMERIC MATERIALS

Plastics and elastomers are commercial products based on polymers (long-chain synthetic organic molecules) that are formulated to obtain specific properties for a particular application. Polymers may be blended together and/or mixed with additives, fillers, or reinforcements to reduce cost, improve heat and light resistance, increase flame retardance, stiffness, toughness, or myriad other physical, chemical, and aesthetic properties. Thus, tens of thousands of commercial products (plastics and elastomers) are derived from a few dozen polymers, with the overwhelming majority being the commodity plastics derived from hydrocarbon monomers continuously obtained from petrochemical feedstocks (i.e., polyolefins and styrenics). The following is a brief introduction to polymers and their chemistry. The interested reader should consult the many excellent texts on polymer science and engineering for more detail.

3.2.1 Monomers, Polymers, and Copolymers

Monomers are reactive liquids or gases that are the building blocks of polymers. Polymers in turn comprise the major component of commercial plastics and elastomers. A single polymer molecule is produced when thousands of liquid or gaseous monomers link together through controlled chemical

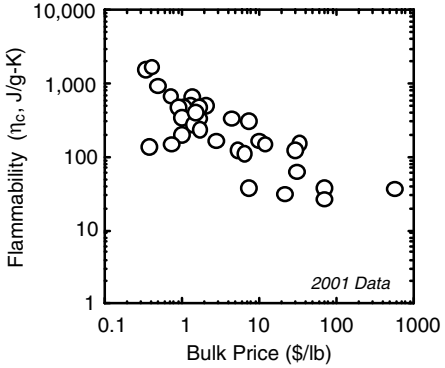

FIGURE 3.1 Flammability (heat release capacity) of plastics versus cost.

reactions called polymerization to produce a long chain. The molecular weight of the polymer increases as additional monomers are added to the chain, with a corresponding increase in boiling point so that the physical state of the reaction mixture changes from a gaseous or liquid monomer to a viscous oil, and finally to a solid. This physical process is reversed in a fire when the chemical bonds in the polymer chain are broken by heat and the polymer reverts back to an oil, liquid, and finally a gas that can mix with oxygen in the flame and undergo combustion (see Fig. 3.6). Thus, the chemical structure of the polymer is closely related to the amount of heat liberated by combustion (see Table 3.3). A detailed description of polymer synthetic chemistry is beyond the scope of this chapter, but a few examples are shown in Fig. 3.2. Generally, polymer molecules are formed when one or more types of monomers add together to form a long chain with practical molar masses ranging from about 50,000 to several million grams per mole. By comparison, the molar mass of automotive gasoline (e.g., octane) is about 100 g/mol. If the monomers react to form a chain without producing any by-products, the polymerization is termed addition, and the chain grows from one end as monomers are sequentially added. Addition polymerization of a single monomer produces a homopolymer such as polyethylene from ethylene gas in Fig. 3.2, while more than one monomer yields a copolymer such as *ethylene-propylene rubber* (EPR), which is an elastomer at room temperature. All of the vinyl polymers and copolymers and most of those containing "ene" in their chemical name (except PBT, PET, PPE, and PPO) in Table 3.1 are addition polymers, as is PA6.

If a small molecule is eliminated during the polymerization, e.g., water is eliminated in the ethylene glycol–terephthalic acid reaction to make *poly(ethyleneterephthalate)* (PET) in Fig. 3.2, then the polymerization is called a condensation polymerization. Condensation polymerization accounts for about half of the polymers in Table 3.1. Engineering plastics (PBT, PET, PPE, PPO, nylons, polysulfones) and many low-cost thermosets (phenolics, aminos, ureas) are condensation polymers.

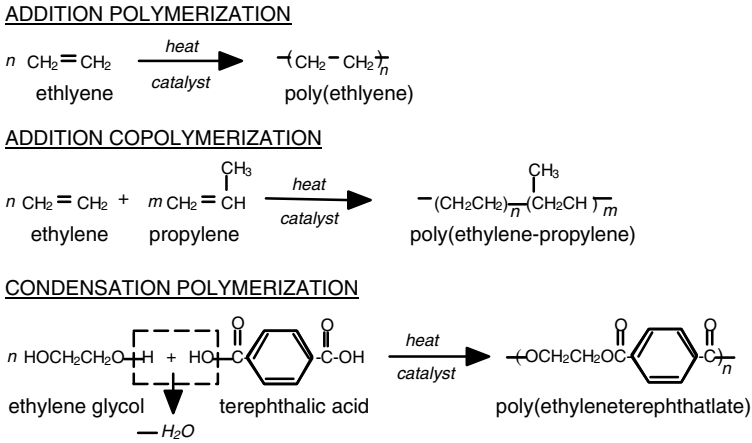

FIGURE 3.2 Examples of plastics made by addition (PE, EPR) and condensation (PET) polymerization.

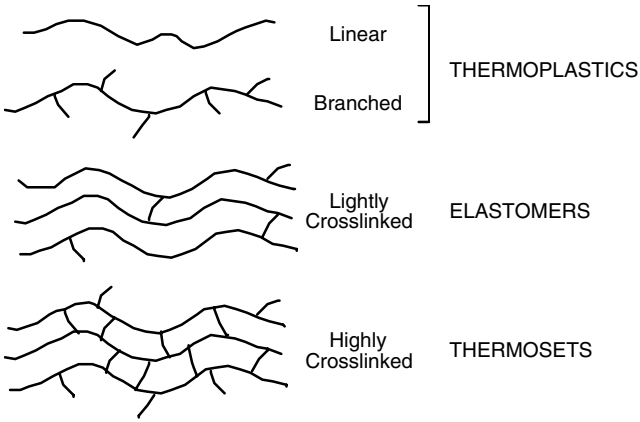

FIGURE 3.3 Molecular architectures for linear, branched, lightly cross-linked, and highly cross-linked plastics and elastomers.

Condensation polymerization involves at least two separate monomers that react together with the elimination of a small molecule that must be continuously removed from the polymerization mixture to achieve high molar mass (thermoplastics) or good structural properties (thermosets).

3.2.2 Polymer Architectures

Molecular. The monomers used to make polymers can have two or more reactive ends or functional groups, $f = 2$, 3, or 4 (typically). Linear polymer chains result if there are two reactive groups ($f = 2$), and linear chains with occasional intramolecular branches or intermolecular cross-links are produced if the average functionality is between 2 and 3 ($f = 2$ to 3). Linear and branched polymer chains can flow when heated and these are called thermoplastics. Lightly cross-linked polymers cannot flow but can be stretched to several times their initial length with instantaneous or delayed recovery depending on whether the polymer is above or below its glass transition temperature, respectively. If the monomers have an average functionality $f > 3$ the result is a highly cross-linked polymer network with a large number of intermolecular chemical bonds. These polymer networks cannot flow when heated and are called thermoset polymers. Fig. 3.3 shows a schematic diagram of these basic molecular architectures. The implication for fire safety of these two types of polymers is that thermoplastics can melt and drip at, or prior to, ignition if they do not char first, and the flaming drips can spread the fire. For this reason the most common flammability test rates plastics for self-extinguishing tendency as well as the propensity to form flaming drips [21]. Thermoset polymers thermally degrade to volatile fuel without dripping and so limit the fire to their own surface.

Supramolecular. Fig. 3.4 shows schematic diagrams of the two basic types of large-scale supramolecular structure of polymers: amorphous and (semi)crystalline. If the polymer chains are linear and the repeat unit (monomer sequence) is asymmetric or highly branched, the polymer chains in bulk are disordered (amorphous), and if there are no fillers or contaminants to scatter visible light, then these materials are usually clear [e.g., Lucite/Plexiglas polymethyl methacrylate, Lexan polycarbonate, flexible PVC, or silicone rubber]. Amorphous polymers have only a single thermal transition corresponding to a second-order thermodynamic transition known as the glass transition temperature T_g. Below the glass transition temperature, the amorphous polymer is a rigid solid, while above T_g, it is a rubber or highly viscous liquid depending on whether it is cross-linked or not. Above the glass transition temperature, there is a 10^6 reduction in stiffness and a change in the slope of density ρ, heat capacity c, and thermal conductivity κ versus temperature. Fig. 3.5 is a schematic plot of dynamic

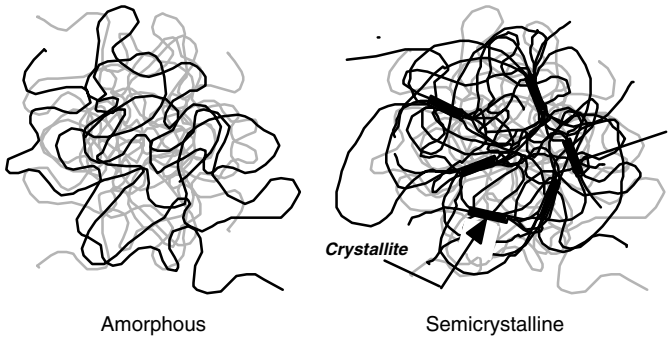

FIGURE 3.4 Amorphous and semicrystalline polymer morphologies.

modulus (stiffness) versus reduced temperature T/T_g showing the dramatic change in stiffness between the glassy state and the rubbery or fluid state. The thermal properties κ, ρ, and c are plotted in reduced form in Fig. 3.5 by normalizing each property p by its value at the glass transition temperature, that is, $p_i(T)/p_i(T_g) = 1$ at $T = T_g$. Fig. 3.5 shows the qualitative changes in κ, ρ, and c with temperature.

If the monomer sequence is fairly regular and symmetric the polymer chain can crystallize into ordered domains known as crystallites that are dispersed in the amorphous (disordered) polymer as illustrated schematically in Fig. 3.4. At the melting temperature T_m, the crystallites melt and the

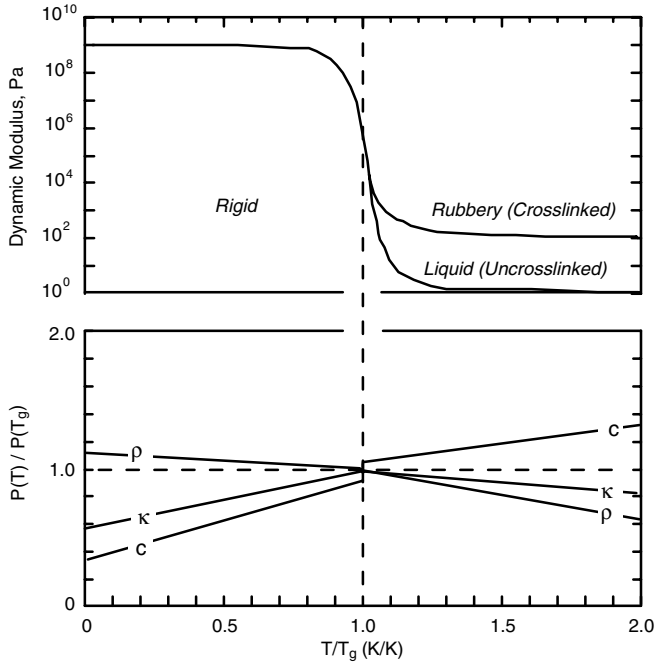

FIGURE 3.5 Dynamic modulus and reduced thermal properties P = κ, ρ, c versus reduced temperature (T/T_g). Slope of κ, ρ, c changes at the glass transition temperature $T = T_g$.

TABLE 3.1 Plastics and Elastomers: Nomenclature, Glass Transition Temperature (T_g), and Melting Temperature (T_m)

Polymer (Common or Trade Name)	Abbreviation	T_g (K)	T_m (K)
Thermoplastics			
Acrylonitrile-butadiene-styrene	ABS	373	—
Cellulose acetate	CA	503	—
Cellulose acetate butyrate	CAB	413	—
Cellulose acetate propionate	CAP	463	—
Cellulose nitrate	CN	—	—
Cellulose proprionate	CP	—	—
Polychlorotrifluoroethylene	CTFE	373	493
Polyethylene-acrylic acid salt (ionomer)	EAA	—	358
Polyethylenechlorotrifluoroethylene	ECTFE		513
Epoxy (PHENOXY-A)	EP	373	—
Epoxy Novolac (PHENOXY-N)	EPN	438	—
Polyethylene-tetrafluoroethylene (TEFZEL)	ETFE	—	543
Ethylene vinyl acetate	EVA	—	378
Fluorinated ethylene propylene	FEP	331	548
Poly(styrene-butadiene)	HIPS	373	—
Poly(p-phenyleneisophthalamide)	KEVLAR	—	820
Polyarylate (liquid crystalline)	LCP	—	603
Poly(m-phenyleneisophthalamide)	NOMEX	—	680
Polytrifluoroethylene	P3FE	304	—
Polyamide 11	PA11	—	475
Polyamide 12	PA12	—	458
Polyamide 6	PA6	313	533
Polyamide 6/10	PA610	—	493
Polyamide 6/12	PA612	—	480
Polyamide 6/6	PA66	323	533
Polyaramidearylester	PAE	—	—
Polyaryletherketone	PAEK	453	—
Polyamideimide (TORLON)	PAI	548	—
Polyacrylonitrile	PAN	368	408
Polyarylate	PAR	463	—
Poly1-butene	PB	249	400
Polybenzimidazole	PBI	698	—
Poly(p-phenylenebenzobisoxazole)	PBO	>900	—
Polybutyleneterephthalate	PBT	313	510
Polycarbonate of bisphenol-A	PC	423	—
Polycarbonate/ABS blend	PC/ABS	398	—
Polyethylene (high density)	PE HD	195	408
Polyethylene (low density)	PE LD	148	373
Polyethylene (medium density)	PE MD	195	396
Polyethylene (crosslinked)	PE XL	195	396
Polyetheretherketone	PEEK	419	607
Polyetherimide (ULTEM)	PEI	486	—
Polyetherketoneketone	PEKK	430	578
Polyethylmethacrylate	PEMA	338	—
Polyethylenenaphthalate	PEN	—	533
Polyethyleneoxide	PEO	213	308
Polyethersulfone (RADEL-A)	PESU	495	—
Polyethyleneterephthalate	PET	342	528
Poly(tetrafluoroethylene-perfluoroether)	PFA	—	583
Polyimide	PI	610	—
Polymethylmethacrylate	PMMA	387	—
Poly(4-methyl-1-pentene)	PMP	303	505
Poly(α-methyl)styrene	PMS	441	—
Polyoxymethylene	POM	204	453
Polypropylene	PP	253	444
Polyphthalamide (AMODEL)	PPA	393	583
Polyphenyleneether	PPE	358	535
Poly(2,6-dimethylphenyleneoxide)	PPO	482	548
Polypropyleneoxide	PPOX	198	—

TABLE 3.1 (*Continued*)

Polymer (Common or Trade Name)	Abbreviation	T_g (K)	T_m (K)
Thermoplastics			
Polyphenylenesulfide	PPS	361	560
Polyphenylsulfone (RADEL-R)	PPSU	492	—
Polystyrene	PS	373	—
Polysulfone	PSU	459	—
Polytetrafluoroethylene	PTFE	240	600
Polytetramethyleneoxide	PTMO	190	320
Polyvinylacetate	PVAC	304	—
Polyvinylbutyral	PVB	324	—
Polyvinylchloride (plasticized/flexible)	PVC (flex)	248	—
Polyvinylchloride (rigid)	PVC (rigid)	354	—
Polyvinylchloride (chlorinated)	CPVC	376	—
Polyvinylidenechloride	PVDC	255	468
Polyvinylidenefluoride	PVDF	233	532
Polyvinylfluoride	PVF	253	503
Polyvinylcarbazole	PVK	423	—
Polyvinylalcohol	PVOH	358	523
Poly(benzoyl-1,4-phenylene) (POLY-X)	PX	433	—
Poly(styrene-acrylonitrile)	SAN	393	—
Elastomers			
Polybutadiene	BDR	175	—
Polyisobutylene (butyl rubber)	BR	214	—
Polyethylene (chlorinated)	CPE	261	—
Polychloroprene (Neoprene)	CR	233	—
Chlorosulfonated polyethylene	CSPE	274	—
Ethylene-propylene-diene	EPDM	224	—
Poly(vinylidenefluouride-hexafluoropropylene)	FKM	255	—
Polypropyleneoxide-allyglycidylether	GPO	198	—
Nitrile-butadiene (Buna-N)	NBR	243	—
Polyisoprene (natural)	NR	203	—
Polyurethane rubber	PUR	223	—
Styrene-butadiene rubber	SBR	240	—
Polydimethylsiloxane (silicone)	SIR	146	—
Thermosets			
Bismaleimide	BMI	573	—
Benzoxazine of bisphenol-A/aniline	BZA	423	—
Cyanate ester of hexafluorobisphenol-A	CEF	546	—
Cyanate ester of bisphenol-A	CEA	543	—
Cyanate ester of bisphenol-E	CEE	548	—
Cyanate ester of bisphenol-M	CEM	528	—
Cyanate ester of tetramethylbisphenol-F	CET	525	—
Diallylphthalate	DAP	423	—
Epoxy	EP	393	—
Melamine formaldehyde	MF	—	—
Phenol formaldehyde	PF	443	—
Polyimide	PI	623	—
Cyanate Ester from Novolac (phenolic triazine)	PT	375	—
PU (isocyanurate/rigid)	PU	—	—
Silicone resin	SI	473	—
Urea formaldehyde	UF	—	—
Unsaturated polyester	UPT	330	—
Vinylester	VE	373	—

entire polymer becomes amorphous and can flow. Because the melting temperature of the crystallites is above the glass transition temperature (typically $T_m/T_g \approx$ 1.3 to 2.0 K/K), crystallinity raises the flow temperature of the plastic and makes it more rigid. However, crystallinity does not prevent flaming drips as the melting temperature is usually much lower than the ignition temperature (compare Tables 3.1 and 3.6). Crystallinity does not exceed 90 to 95 percent in bulk polymers, with 20 to 80 percent being typical, because the polymer chains are too long to pack into an orderly crystal lattice without leaving some dangling ends that segregate into disordered (amorphous) domains. Crystallites usually are of sufficient size to scatter visible light so that natural/unfilled semicrystalline plastics are translucent or white. Semicrystalline polymers of commercial importance include polyethylene, polypropylene, PET, polytetrafluoroethylene, and the polyamides (nylons).

3.2.3 Commercial Materials

Table 3.1 lists some plastics and elastomers for which a reasonably complete set of fire and thermal properties were available. Abbreviations conform to the recommended International Standards Organization (ISO) 1043-1 (thermoplastics and thermosets) and ASTM D1418 (elastomers) designations. The following definitions apply to the commercial plastics and elastomers in this chapter:

Thermoplastic. A linear or branched polymeric solid that flows with the application of heat and pressure at the glass transition temperature (amorphous) or the crystalline melting temperature (semicrystalline), whichever is higher. Different thermoplastics can be blended together in the molten state to obtain new compositions, called alloys, with improved toughness (PC/ABS, HIPS), better high-temperature properties (PS/PPO), or better flame retardancy (PVC/PMMA). Reinforced thermoplastic grades typically contain chopped fiberglass or carbon fibers at 30 to 40 percent by weight to increase strength and stiffness. Continuous sheet and profile are made by extrusion, and individual parts and shapes by injection molding, rotational molding, etc.

Elastomer. A lightly cross-linked linear polymer that is above its glass transition temperature at room temperature (i.e., is rubbery). Elastomers exhibit high extensibility (>100 percent strain) and complete, instantaneous recovery. Cross-linking can be by permanent chemical bonds (thermoset), which form in a process called vulcanization, or by thermally labile glassy or ionic domains that can flow with the application of heat (thermoplastic elastomer). Commercial elastomers are typically compounded with oils, fillers, extenders, and particulate reinforcement (carbon black, fumed silica). Vulcanized elastomers (e.g., tires) are cured in closed heated molds, while thermoplastic elastomers can be extruded, compression molded, or injection molded.

Thermoset. A rigid polymer made from two or more multifunctional monomers. Polymerization to a highly cross-linked network gives the final form (typically in a mold) that will not flow with application of heat or pressure. Thermoset polymers degrade thermally rather than flow because the intermolecular bonds are permanent chemical ones. Thermosets are typically brittle and commercial formulations are usually compounded with chopped fiberglass or mineral fillers to improve strength and reduce cost.

The generic fire property data tabulated in this chapter for plastics and elastomers are averages of values within sources and between sources (typically 1 to 3) for each material unless the values differed by more than about 20 percent, in which case the range is specified. No attempt was made to establish the composition of commercial products reported in the literature and nominal values are used throughout. The tabulated fire and thermal properties are thus representative of the average of commercial formulations. Polymeric materials listed by name (e.g., polyethylene terephthalate/PET) are assumed to be natural (unmodified) polymers, copolymers, and blends containing at most a few weight percent of stabilizers and processing aids. Flame-retardant grades are designated by the suffix -FR which usually refers to an additive level sufficient to achieve a self-extinguishing rating in a bunsen burner test of ignition resistance, e.g., Underwriters Laboratory test for flammability of plastic materials (UL 94) [21]. Flame-retardant formulations are proprietary but can include inert fillers

such as alumina trihydrate (ATH) and flame-retardant chemicals [7, 9, 10, 13, 17]. Thermoplastics, thermosets, and elastomers reinforced with chopped glass fibers are designated by the suffix -G. Reinforcement level is 30 to 40 percent by weight unless otherwise noted. Filled grades designated by the suffix -M contain mineral fillers such as talc, calcium carbonate, etc., at unspecified levels.

3.2.4 Thermodynamic Quantities

Thermal Properties. The rate at which heat is transported and stored in polymers in a flame or fire is of fundamental importance because these processes determine the time to ignition and burning rate. There are no good theories to predict the thermal conductivity κ (W/m·K), heat capacity c (kJ/kg·K), or density ρ(kg/m^3) of condensed phases (e.g., solid or molten polymers) from chemical structure, but empirical structure-property correlations have been developed that allow calculation of thermal properties from additive atomic [29] or chemical group [30] contributions if the chemical structure of the plastic is known. Table 3.2 lists generic thermophysical properties at 298 K gathered from the literature [22–33, 35–39] for a number of common thermoplastics, thermoset resins, elastomers, and fiberglass-reinforced plastics. Entries are individual values, averages of values from different sources, or averages of a range of values from a single source, and therefore represent in most cases a generic property value with an uncertainty of about 10 to 20 percent. Empirical structure-property correlations [29, 30] were used to calculate thermal properties of several polymers at 298 K from their chemical structure when these could not be found in the literature. The general trend of κ, ρ, and c with temperature is shown in reduced form in Fig. 3.5 relative to the values of these properties at the glass transition temperature.

Thermal conductivity increases with degree of crystallinity and the temperature dependence of the thermal conductivity of polymers varies widely in the literature [31–33]. However, a rough approximation of temperature dependence of the thermal conductivity relative to its value at the glass transition temperature $\kappa(T_g)$ is [29, 30]

$$\kappa \approx \kappa(T_g)\left[\frac{T}{T_g}\right]^{0.22} \quad (T < T_g) \tag{3.1a}$$

$$\kappa \approx \kappa(T_g)\left\{1.2 - 0.2\left[\frac{T}{T_g}\right]\right\} \quad (T > T_g) \tag{3.1b}$$

The relationship between density and temperature can be expressed (neglecting the abrupt change on melting of semicrystalline polymers) to a first approximation [30]

$$\frac{1}{\rho} = \frac{1}{\rho_0} + B(T - T_0) \tag{3.2}$$

where $\rho = \rho(T)$ is the density at temperature T, ρ_0 is the density at temperature $T_0 = 298$ K, and $B = 5 \pm 2 \times 10^{-7}$ m^3/(kg·K) is the volume thermal expansivity per unit mass. Neglecting crystalline melting, the temperature dependence of the heat capacity can be approximated [29, 30]

$$c = (c_0 + \Delta c)(0.64 + 1.2 \times 10^{-3}T) \approx \frac{3}{4}c_0(1 + 1.6 \times 10^{-3}T) \tag{3.3}$$

where $c = c(T)$ in units of kJ/kg·K is the heat capacity at temperature T, c_0 is the heat capacity at standard temperature $T_0 = 298$ K, and Δc is the change in heat capacity at the glass transition temperature.

The product $\kappa\rho c$ is a quantity called the thermal inertia that emerges from the transient heat transfer analysis of ignition time [see Eq. (3.52)]. The individual temperature dependence of κ, ρ, and c revealed by Eqs. (3.1) through (3.3) and experimental data for about a dozen plastics [22–39] suggest that the product of these terms (i.e., the thermal inertia) should have the approximate temperature dependence:

$$\kappa\rho c(T) \approx \kappa_0\rho_0 c_0 T/T_0 = (\kappa\rho c)_0 T/T_0 \tag{3.4}$$

where κ_0, ρ_0, c_0 are the room temperature (T_0) values listed in Table 3.2. Another thermal parameter that emerges from unsteady heat transfer analyses [see Eqs. (3.52) and (3.58)] is the thermal diffusivity $\alpha = \kappa/\rho c$. Thermal diffusivities of polymers at T_0 reported in the literature [26–33] or calculated from κ, ρ, and c are listed in the last column of Table 3.2. Thermal diffusivity generally decreases with temperature according to the approximate relationship derived from experimental data [32, 33]

$$\alpha(T) = \alpha_0 T_0/T$$

Heat of Combustion (HOC). At constant pressure and when no nonmechanical work is done, the heat (Q, q) and enthalpy (H, h) of a process are equal. The flaming combustion of polymers at atmospheric pressure satisfies these conditions. The high-pressure adiabatic combustion of a polymer in a bomb calorimeter satisfies these conditions approximately, since the fractional pressure change is small. Consequently, the terms heat and enthalpy are used interchangeably in polymer combustion. Heats of combustion of organic macromolecules can be calculated from the oxygen consumed in the combustion reaction [40–45]. Oxygen consumption is, in fact, the basis for most modern bench- and full-scale measurements of heat release in fires [41, 42]. The principle of oxygen consumption derives from the observation that for a wide range of organic compounds, including polymers, the heat of complete combustion per mole of oxygen consumed is a constant E that is independent of the composition of the polymer. Mathematically,

$$E = h_{c,p}^{O}\left[\frac{nM}{n_{O_2}M_{O_2}}\right] = \frac{h_{c,p}^{O}}{r_O} = 13.1 \pm 0.7 \text{ kJ/g O}_2 \tag{3.5}$$

where $h_{c,p}^{\circ}$ is the net heat of complete combustion of the polymer solid with all products in their gaseous state, n and M are the number of moles and molecular weight of the molecule or polymer repeat unit, respectively, n_{O_2} is the number of moles of O_2 consumed in the balanced thermochemical equation, and $M_{O_2} = 32$ g/mol is the molecular weight of diatomic oxygen. In Eq. (3.5), the quantity $r_O = [n_{O_2}M_{O_2}/nM]$ is the oxygen-to-fuel mass ratio.

To illustrate the thermochemical calculation of the net HOC we use as an example poly(methylmethacrylate) (PMMA), which has the chemical structure

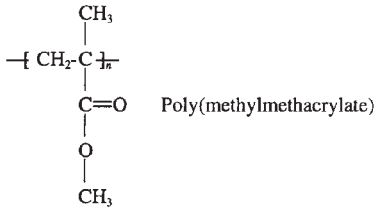

The methylmethacrylate repeat unit shown in brackets has the atomic composition $C_5H_8O_2$ so the balanced chemical equation for complete combustion is

$$C_5H_8O_2 + 6\ O_2 \rightarrow 5\ CO_2 + 4\ H_2O$$

Thus, 6 moles of O_2 are required to completely convert 1 mole of PMMA repeat unit to carbon dioxide and water. Inverting Eq. (3.5)

$$h_{c,p}^{O} = E\left[\frac{n_{O_2}M_{O_2}}{nM}\right] = \frac{(13.1 \text{ kJ/g O}_2)(6 \text{ mol O}_2)(32 \text{ g O /m}_2\text{ol O}_2)}{(1 \text{ mol PMMA})(100 \text{ g/mol PMMA})} = 25.15 \text{ kJ/g}$$

Table 3.3 lists net heats of complete combustion for plastics and elastomers obtained from the literature [39–41]. Values in parentheses were calculated from the elemental composition as illustrated above.

Heat of Gasification. In principle, the heat (enthalpy) of gasification is the difference between the enthalpy of the solid in the initial state and the enthalpy of the volatile thermal-decomposition products

TABLE 3.2 Thermal Properties of Plastics

Polymer	κ W/m·K	ρ kg/m^3	c_p kJ/kg·K	α m^2/s $\times$ 10^7
ABS	0.26	1050	1.50	1.65
BDR	0.22	970	1.96	1.16
BR	0.13	920	1.96	0.72
CA	0.25	1250	1.67	1.20
CAB	0.25	1200	1.46	1.43
CAP	0.25	1205	1.46	1.42
CE	0.19	1230	1.11	1.39
CN	0.23	1375	1.46	1.15
CP	0.20	1300	1.46	1.05
CPVC	0.48	1540	0.78	4.00
CR	0.19	1418	1.12	1.20
CTFE	0.23	1670	0.92	1.50
DAP	0.21	1350	1.32	1.18
DAP-G	0.42	1800	1.69	1.38
EAA	0.26	945	1.62	1.70
ECTFE	0.16	1690	1.17	0.81
EP	0.19	1200	1.7	1.12
EPDM	0.20	930	2.0	1.08
EP-G	0.42	1800	1.60	1.46
EPN	0.19	1210	1.26	1.25
ETFE	0.24	1700	1.0	0.66
EVA	0.34	930	1.37	2.67
FEP	0.25	2150	1.17	0.99
HIPS	0.22	1045	1.4	1.54
LCP	0.20	1350	1.20	1.24
MF	0.25	1250	1.67	1.20
MF-G	0.44	1750	1.67	1.51
NBR	0.25	1345	1.33	1.40
NR	0.14	920	1.55	0.98
P3FE	0.31	1830	1.08	1.41
PA11	0.28	1120	1.74	1.44
PA11-G	0.37	1350	1.76	1.56
PA12	0.25	1010	1.69	1.46
PA6	0.24	1130	1.55	1.37
PA610	0.23	1100	1.51	1.38
PA612	0.22	1080	1.59	1.28
PA66	0.23	1140	1.57	1.29
PA6-G	0.22	1380	1.34	1.19
PAEK	0.30	1300	1.02	2.27
PAI	0.24	1420	1.00	1.69
PAN	0.26	1150	1.30	1.74
PAR	0.18	1210	1.20	1.24
PB	0.22	920	2.09	1.14
PBI	0.41	1300	0.93	3.40
PBT	0.22	1350	1.61	1.01
PC	0.20	1200	1.22	1.36
PC-G	0.21	1430	1.10	1.34
PE (HD)	0.43	959	2.00	2.24
PE (LD)	0.38	925	1.55	2.65
PE (MD)	0.40	929	1.70	2.53

TABLE 3.2 (*Continued*)

Polymer	κ W/m·K	ρ kg/m^3	c_p kJ/kg·K	α m^2/s × 10^7
PEEK	0.20	1310	1.70	0.90
PEI	0.23	1270	1.22	1.48
PEKK	0.22	1280	1.00	1.72
PEMA	0.18	1130	1.47	1.08
PEO	0.21	1130	2.01	0.90
PESU	0.18	1400	1.12	1.15
PET	0.20	1345	1.15	1.29
PET-G	0.29	1700	1.20	1.42
PF	0.25	1300	1.42	1.35
PFA	0.25	2150	1.0	1.16
PF-G	0.40	1850	1.26	1.72
PI	0.11	1395	1.10	0.72
PI-TS	0.21	1400	1.13	1.33
PMMA	0.20	1175	1.40	1.19
PMP	0.17	834	1.73	1.18
PMS	0.20	1020	1.28	1.53
POM	0.23	1420	1.37	1.18
PP	0.15	880	1.88	0.89
PPA	0.15	1170	1.40	0.92
PPE	0.23	1100	1.19	1.76
PPO	0.16	1100	1.25	1.16
PPO-G	0.17	1320	1.31	0.98
PPS	0.29	1300	1.02	2.19
PPSU	0.18	1320	1.01	1.35
PS	0.14	1045	1.25	1.04
PS-G	0.13	1290	1.05	0.96
PSU	0.26	1240	1.11	1.89
PTFE	0.25	2150	1.05	1.11
PU	0.21	1265	1.67	0.99
PUR	0.19	1100	1.76	0.98
PVAC	0.16	1190	1.33	1.03
PVC (flex)	0.17	1255	1.38	0.98
PVC (rigid)	0.19	1415	0.98	1.34
PVDC	0.13	1700	1.07	0.91
PVDF	0.13	1760	1.12	0.68
PVF	0.13	1475	1.30	0.72
PVK	0.16	1265	1.23	1.02
PVOH	0.20	1350	1.55	0.96
PX	0.32	1220	1.3	2.02
SAN	0.15	1070	1.38	1.02
SBR	0.17	1100	1.88	0.82
SI-G	0.30	1900	1.17	1.35
SIR	0.23	970	1.59	1.49
UF	0.25	1250	1.55	1.29
UPT	0.17	1230	1.30	1.06
UPT-G	0.42	1650	1.05	1.85
VE	0.25	1105	1.30	1.74

TABLE 3.3 Net Heats of Complete Combustion and Chemical Formulae of Plastics (Calculated Values in Parentheses. Averages Indicated by ±1 Standard Deviation)

Polymer	Chemical formula	Net heat of complete combustion MJ/kg
ABS	$C_{15}H_{17}N$	36.0 ± 3.0
BMI	$C_{21}H_{14}O_4N_2$	(26.3)
BR	C_4H_8	42.7
BZA	$C_{31}H_{30}O_2N_2$	33.5
CA	$C_{12}H_{16}O_8$	17.8
CAB	$C_{12}H_{18}O_7$	22.3
CAP	$C_{13}H_{18}O_8$	(18.7)
CEA	$C_{17}H_{14}O_2N_2$	28.8
CEE	$C_{16}H_{12}O_2N_2$	28.4
CEF	$C_{16}H_{12}O_2N_2$	18.3
CEM	$C_{26}H_{24}O_2N_2$	33.1
CEN	$C_{24}H_{15}O_3N_3$	28.8 ± 1.4
CET	$C_{19}H_{18}O_2N_2$	30.0
CN	$C_{12}H_{17}O_{16}N_3$	10.5 ± 3.1
CP	$C_{15}H_{22}O_8$	(21.0)
CPE (25% Cl)	$C_{10}H_{19}Cl$	31.6
CPE (36% Cl)	C_4H_7Cl	26.3
CPE (48% Cl)	$C_8H_{18}Cl_3$	20.6
CPVC	CHCl	12.8
CR	C_4H_5Cl	18.6 ± 8.9
CSPE	$C_{282}H_{493}Cl_{71}SO_2$	26.7
CTFE	C_2ClF_3	5.5 ± 3.5
DAP	$C_7H_7O_2$	26.2
EAA	C_5H_8O	(32.4)
ECTFE	$C_4H_4F_3Cl$	13.6 ± 1.9
EP	$C_{21}H_{24}O_4$	32.0 ± 0.8
EPDM	C_5H_{10}	38.5
EPN	$C_{20}H_{11}O$	29.7
ETFE	$C_4H_4F_4$	12.6
EVA	C_5H_9O	(33.3)
FEP	C_5F_{10}	7.7 ± 4.0
FKM	$C_5H_2F_8$	12.5 ± 2.5
HIPS	$C_{14}H_{15}$	42.5
KEVLAR	$C_{14}H_{10}O_2N_2$	(27.3)
LCP	$C_{39}H_{22}O_{10}$	25.8
MF	$C_6H_9N_6$	18.5
NBR	$C_{10}H_{14}N$	33.1 ± 0.4
NOMEX	$C_{14}H_{10}O_2N_2$	26.5 ± 1.2
NR	C_5H_8	42.3
P3FE	C_2HF_3	(11.9)
PA11	$C_{11}H_{21}ON$	34.5
PA12	$C_{12}H_{23}ON$	(36.7)
PA6	$C_6H_{11}ON$	28.8 ± 1.1
PA610	$C_{16}H_{30}O_2N_2$	(33.4)
PA612	$C_{18}H_{34}O_2N_2$	(34.5)
PA66	$C_{12}H_{22}O_2N_2$	30.6 ± 1.8
PAEK	$C_{13}H_8O_2$	30.2
PAI	$C_{15}H_8O_3N_2$	24.3
PAN	C_3H_3N	31.0
PAR	$C_{23}H_{18}O_4$	(29.9)
PB	C_4H_9	43.4
PBD	C_4H_6	42.8

TABLE 3.3 (*Continued*)

Polymer	Chemical formula	Net heat of complete combustion MJ/kg
PBI	$C_{20}H_{12}N_4$	21.4
PBO	$C_{14}H_6O_2N_2$	28.6
PBT	$C_{12}H_{12}O_4$	26.7
PC	$C_{16}H_{14}O_3$	30.4 ± 0.8
PC/ABS	$C_{45}H_{43}O_6N$	(32.4)
PE (HD)	C_2H_4	43.8 ± 0.7
PE (LD)	C_2H_4	(44.8)
PE (MD)	C_2H_4	(44.8)
PEEK	$C_{19}H_{12}O_3$	30.7 ± 0.6
PEI	$C_{37}H_{24}O_6N_2$	29.0 ± 1.0
PEKK	$C_{20}H_{12}O_3$	30.3
PEMA	$C_6H_{10}O_2$	(27.6)
PEN	$C_{14}H_{10}O_4$	(25.2)
PEO	C_2H_4O	24.7
PESU	$C_{12}H_8O_3S$	24.9 ± 0.4
PET	$C_{10}H_8O_4$	22.2 ± 1.4
PF	C_7H_5O	28.6
PFA	C_5OF_{10}	5.0
PI	$C_{22}H_{10}O_5N_2$	25.4
PMMA	$C_5H_8O_2$	25.0 ± 0.1
PMP	C_6H_{12}	43.4
PMS	C_9H_{10}	40.4
POM	CH_2O	15.7 ± 0.2
PP	C_3H_6	43.1 ± 0.4
PPA	$C_{14}H_{19}O_2N_2$	(30.1)
PPE	C_6H_4O	(29.6)
PPO	C_8H_8O	32.9 ± 0.3
PPOX	C_3H_6O	28.9
PPS	C_6H_4S	28.3 ± 0.7
PPSU	$C_{24}H_{16}O_4S$	27.2
PS	C_8H_8	40.5 ± 1.3
PSU	$C_{27}H_{22}O_4S$	29.2 ± 0.3
PTFE	C_2F_4	6.0 ± 0.7
PTMO	C_4H_8O	31.9
PU	$C_6H_8O_2N$	24.3 ± 2.1
PUR	$C_{80}H_{120}O_2N$	26.3 ± 2.5
PVAC	$C_4H_6O_2$	21.5
PVB	$C_8H_{14}O_2$	30.7
PVC (flex)	$C_{26}H_{39}O_2Cl$	24.7 ± 3.5
PVC (rigid)	C_2H_3Cl	16.7 ± 0.4
PVDC	$C_2H_2Cl_2$	13.1 ± 4.9
PVDF	$C_2H_2F_2$	13.7 ± 0.6
PVF	C_2H_3F	20.3
PVK	$C_{14}H_{11}N$	(36.4)
PVOH	C_2H_4O	22.2 ± 1.2
PX	$C_{13}H_8O$	37.4
SAN	$C_{27}H_{27}N$	(38.8)
SBR	$C_{10}H_{13}$	42.0
SI	$C_{12}H_{10}O_3Si_2$	(24.4)
SIR	C_2H_6OSi	17.1 ± 3.0
UF	$C_3H_6O_2N_2$	20.8 ± 8.7
UPT	$C_{12}H_{13}O_3$	24.4 ± 5.8
VE	$C_{29}H_{36}O_8$	(27.8)

at the pyrolysis temperature. Thus, the heat of gasification is expected to be a thermodynamic quantity comprised of the sum of the enthalpies required to bring the polymer from the solid state at the initial (room) temperature T_0 and pressure P_0 (1 atm) to the gaseous state at the pyrolysis temperature and pressure T_p and P_0, respectively. If the stored heat on a molar basis is ΔH_s, the enthalpy of fusion (melting) for semicrystalline polymers is ΔH_f, the bond dissociation enthalpy is ΔH_d, and the enthalpy of vaporization of the decomposition products is ΔH_v, then the molar heat of gasification is

$$\Delta H_g = \Delta H_s + \Delta H_f + \Delta H_d + \Delta H_v \tag{3.6}$$

Table 3.4 illustrates the magnitude of these enthalpic terms on a mass basis for amorphous poly(methylmethacrylate), polystyrene, and semicrystalline polyethylene. Values in joules per gram (J/g) are obtained by dividing the molar heat by the molecular weight of the gaseous decomposition products M_g. The stored heat Δh_s was obtained by numerical integration of heat capacity versus temperature [35] from ambient to the dissociation temperature. Unfortunately, experimental data for c versus T for polymers is scarce, but a reasonable approximation for the stored heat is obtained by integrating the analytic expression for the heat capacity [Eq. (3.2)] between room temperature (T_0) and the onset degradation temperature (T_d)

$$\Delta h_s = \int_{T_0}^{T_d} c(T)\,dT = \frac{3}{4}c_0\left\{(T_d - T_0) + 0.8 \times 10^{-3}\,\frac{T_d^2}{T_0^2}\right\} \approx \frac{3}{4}c_0(T_d - T_0) \tag{3.7}$$

where c_0 and T_d are calculable from the polymer chemical structure using empirical molar group contributions [29, 30]. The dissociation (bond-breaking) enthalpy Δh_d is assumed to be equal to the heat of polymerization but opposite in sign for these polymers that thermally degrade by random or end-chain scission [34] (see Table 3.5). The degradation product for polyethylene is assumed to be a tetramer (i.e., octane with $M_g = 112$ g/mol) for the purpose of calculating the heats of dissociation and vaporization on a mass basis for this polymer, and the degree of polyethylene crystallinity is taken to be 90 percent. All other enthalpies in Table 3.4 were obtained from handbooks [35] using monomer molecular weights M to convert the energies to a mass basis. The values for h_g in the second to last row were obtained by summing the individual enthalpies according to Eq. (3.6) for each polymer.

In practice, the heat of gasification per unit mass of solid h_g is rarely calculated because detailed and reliable thermodynamic data for the polymer and its decomposition products are generally unavailable except for the most common polymers. Direct laboratory measurement of h_g using differential thermal analysis and differential scanning calorimetry have been reported, but h_g is usually measured in a constant heat flux gasification device or fire calorimeter. In these experiments a plot of mass loss rate per unit surface area (mass flux) versus external heat flux has slope $1/L_g$ where

$$L_g = \frac{h_g}{1 - \mu} \tag{3.8}$$

TABLE 3.4 Components of the Heat of Gasification of PMMA, PS, and PE

Polymer	PMMA	PS	PE
Monomer MW (g/mole)	100	104	28
Fuel MW (g/mole)	100	104	112
Δh_s(J/g)	740	813	803
Δh_f(J/g)	amorphous	amorphous	243
Δh_d(J/g)	550	644	910
Δh_v(J/g)	375	387	345
$h_g = \sum \Delta h_i$(J/g)	1665	1850	2301
h_g (measured) J/g	1700	1800	2200

is the heat absorbed per unit mass of volatile fuel produced and μ is the nonfuel fraction (char or inert filler). The last row in Table 3.4 lists the average of h_g values for these noncharring polymers (see Table 3.11). Agreement is seen to be quite good between experimental values and thermochemical calculations of h_g. Table 3.11 in the section on "Steady Burning" contains L_g values for about 75 plastics, thermosets, and elastomers.

3.3 THE BURNING PROCESS

3.3.1 The Fire Triangle

Strictly speaking, solid polymers do not burn. Rather, it is their volatile thermal decomposition products that burn in the gas phase when mixed with oxygen and ignited. Ignition occurs when the concentration of volatile fuel gases reaches the lower flammability limit for the particular fuel-air mixture. Polymers do not burn in the condensed state because of the low solubility and diffusivity of oxygen and the low oxidation rate at the decomposition temperature. In fact, thermal degradation of the surface layer of polymer in the presence of a heat source is thought to occur in a reducing, rather than an oxidizing, environment. Low-molecular-weight volatile organic compounds are produced that mix with atmospheric oxygen above the polymer surface to form a flammable mixture that, when ignited, combusts, producing a luminous flame. The surface temperature of the burning plastic cannot greatly exceed its thermal decomposition temperature until all of the volatile fuel is depleted because until this occurs excess thermal energy is consumed by vaporization (mass transfer) of the volatile fuel rather than being stored in the solid as a temperature rise. The surface temperature of plastics at ignition, also called the fire point temperature, should therefore be close to the thermal degradation temperature (see Table 3.6). At these temperatures, the thermal degradation reactions at the plastic surface are faster than the rate at which heat is absorbed. Consequently, it is the latter process (i.e., heat transfer) that governs the burning rate, heat release rate, and smoke evolution during flaming combustion. The chemical structure of the plastic or elastomer determines the thermal stability (ignition temperature), fuel fraction, potential HOC of the fuel gases, and the products of combustion.

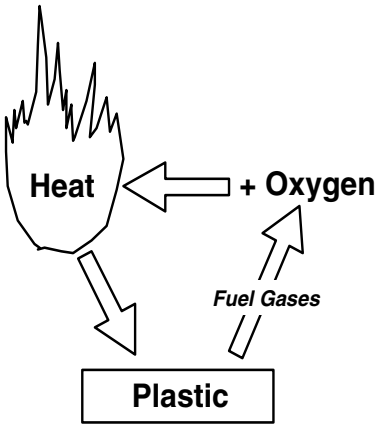

FIGURE 3.6 The fire triangle. Heating of the plastic generates volatile thermal degradation products (fuel gases) that mix with air forming a combustible mixture. Ignition of the combustible mixture releases heat that continues the burning process.

Fig. 3.6 illustrates the three coupled processes required for flaming combustion: (1) heating of the polymer, (2) thermal decomposition of the solid polymer to gaseous fuel, and (3) ignition and combustion of the fuel gases in air. An ignition source or thermal feedback of radiant energy from the flame supplies heat to the polymer surface that causes thermolysis of primary chemical bonds in the polymer molecules. Evaporation of the low-molar-mass degradation products and the reaction of these with air (oxygen) in the combustion zone above the surface releases heat and produces carbon dioxide, water, and incomplete combustion products such as carbon monoxide, mineral acids, unburned hydrocarbons, and soot. In order to resist burning, the fire cycle must be broken at one or more places.

Several comprehensive texts have been written on the chemistry and physics of gas phase combustion [18–20]. In contrast, combustible solids (with the exception of wood) have received relatively little attention. The remainder of this chapter examines the flaming combustion of solids, specifically plastics, from a phenomenological perspective. Recent developments in the metrology and modeling of fire and its impact on materials provide the basis for relating polymer ignition

and burning to measurable, macroscopic flammability parameters. Connecting these macroscopic flammability parameters to the kinetics and thermodynamics of the fuel-generation process provides a thermochemical basis for the solid-state processes of flaming combustion.

3.3.2 Chemical Changes during Burning

The elementary fuel-generation step of a solid in a fire is thermal degradation [46–63]. Typically, it is the fraction and rate of production of volatile fuel at fire temperatures and the HOC of this fuel that determine the flammability of plastics and elastomers. Short-term thermal stability and reduced fuel fraction (increased char yield) are achieved by eliminating hydrogen atoms from the polymer molecule so that recombination of carbon radicals to form char during thermal degradation is kinetically favored over hydrogen abstraction/termination reactions that produce volatile fuel fragments. A low HOC is observed when heteroatoms (e.g., halogens, nitrogen, phosphorus, sulfur, silicon, boron, and oxygen) replace carbon and hydrogen in the polymer molecule. Heteroatoms form stable gas phase combustion products that are either low in fuel value (i.e., N_2, SO_2, hydrogen halides) or thermally stable solid oxides (i.e., SiO_2, P_2O_5, B_2O_3) that precipitate onto the polymer surface and act as mass- and thermal-diffusion barriers.

Thermal Decomposition of the Solid. The basic thermal degradation mechanism leading to volatile fuel generation in polymers involves primary and secondary decomposition events. The primary decomposition step can be main-, end-, or side-chain scission of the polymer [5, 46–48]. Subsequent thermal degradation reactions depend largely on the chemical structure of the polymer but typically proceed by hydrogen transfer to α- or β-carbons, nitrogen or oxygen, intramolecular exchange (cyclization), side-chain reactions, small-molecule (SO_2, CO_2, S_2) elimination, molecular rearrangement, and/or unzipping to monomer [5, 46–48, 51]. Unzipping or depolymerization of vinyl polymers is characterized by a kinetic chain length or "zip length," which is the average number of monomer units produced by a decomposing radical before the radical is deactivated by termination or transfer. Mathematically, the zip length is the ratio of the rate constants for initiation to termination. Aromatic backbone polymers such as polycarbonate, polyimide, and polyphenyleneoxide tend to decompose in varying degrees to a carbonaceous char residue through a complex set of reactions involving cross-linking and bond scission [7]. A generally applicable, detailed mechanism for thermal degradation of aromatic polymers is unlikely.

The enthalpy of the solid → gas phase change has been related to the global activation energy for pyrolysis E_a measured in a laboratory *thermogravimetric analyzer* (TGA) [34, 52]. In particular, the average molecular weight of the decomposition products M_g is related to the heat of gasification per unit mass of solid h_g

$$h_g = \frac{E_a}{M_g} \tag{3.9}$$

In this case, the average molar mass of the decomposition products M_g and the molar mass of the monomer or repeat unit M should be in the ratio

$$\frac{M_g}{M} = \frac{E_a}{M h_g} \tag{3.10}$$

Polymers that pyrolyze to monomer by end-chain scission (depolymerize/unzip) at near-quantitative yield such as PMMA, polyoxymethylene, and polystyrene should have M_g equal to the monomer molar mass M, that is, $M_g/M \approx 1$. Polymers such as polyethylene and polypropylene that decompose by main-chain scission (cracking) to multimonomer fragments have $M_g/M > 1$. In contrast, polymers with complex molecular structures and high molar mass repeat units ($M \geq 200$ g/mol) such as nylon, cellulose, or polycarbonate degrade by random scission, cyclization, small-molecule splitting, or chain stripping of pendant groups (e.g., polyvinylchloride) and yield primarily low-molar-mass species (water, carbon dioxide, alkanes, mineral acids) relative to the starting monomer so that $M_g/M < 1$. Table 3.5 shows fuel/monomer molar mass ratios M_g/M calculated as E_a/Mh_g according to

TABLE 3.5 Heats of Gasification, Pyrolysis Activation Energy, Char Yield, and Calculated Molecular Weight of Decomposition Products for Some Polymers

Polymer	M (g/mol)	L_g (kJ/g)	μ (g/g)	h_g (kJ/g)	E_a (kJ/mol)	M_g/M	Pyrolysis products
				Chain cracking			
PP	42	1.9	0	1.9	243	3.0	C_2–C_{90} saturated and unsaturated hydrocarbons
PE	28	2.2	0	2.2	264	4.3	
				Unzipping			
PS	104	1.8	0	1.8	230	1.2	40–60% monomer
PMMA	100	1.7	0	1.7	160	0.94	100% monomer
POM	30	2.4	0	2.4	84	1.2	100% monomer
				Intramolecular scission			
PA 66	226	2.1	0	2.1	160	0.3	H_2O, CO_2, C_5 HC's
PVC	62	2.7	0.1	2.4	110	0.7	HCl, benzene, toluene
Cellulose	162	3.2	0.2	2.6	200	0.5	H_2O, CO_2, CO
PT	131	5.0	0.6	2.0	178	0.3	Complex mixture of low molecular weight products
PC	254	2.4	0.3	1.7	200	<1	
PEI	592	3.5	0.5	1.8	≈275	<1	
PPS	108	3.8	0.5	1.9	≈275	<1	
PEEK	288	3.4	0.5	1.7	≈275	<1	
PAI	356	4.8	0.6	1.9	≈275	<1	
PX	180	6.4	0.7	1.9	≈275	<1	

Eq. (3.10) for some of the commercial polymers listed in Tables 3.1 to 3.4. Global pyrolysis activation energies for the thermally stable engineering plastics listed in the last four rows of Table 3.5 are estimated to be in the range $E_a = 275 \pm 25$ kJ/mol [30, 35, 47, 49]. Qualitative agreement is observed between the modes of pyrolysis (end-chain scission, random scission, chain stripping) and the calculated fragment molecular weight using Eq. (3.10), suggesting that the global pyrolysis activation energy determined from mass loss rate experiments is the molar enthalpy of pyrolysis of the degradation products. Surprisingly, the heat of gasification per unit mass of solid $h_g = (1-\mu)L_g$ remains constant at about 2.0 kJ/g over this broad range of thermal stability and decomposition modes.

Phenomenological schemes that account for some or all of the pyrolysis products of combustible solids (gas, tar, primary char, secondary char, secondary gas) have been proposed [46–63] wherein the decomposition steps occur sequentially (series), simultaneously (parallel), or in some combination of series/parallel steps. All of the models predict rate-dependent peak decomposition temperatures. A simple solid-state fuel-generation model that shows reasonable agreement with thermal analysis data [50, 52], numerical models of fire behavior [63], and experimental data [63] is

$$\text{Polymer Solid, } P \underset{k_r}{\overset{k_i}{\rightleftarrows}} \text{Reactive Intermediate, } I^* \begin{cases} \xrightarrow{k_g} \text{Fuel Gases, } G\ (\uparrow) \\ \xrightarrow{k_c} \text{Char, } C \end{cases}$$

in which the thermal degradation of polymer mass P is assumed to occur in a single step involving rapid equilibrium between the polymer and an active intermediate I^* that simultaneously produces gas G and char C. Fig. 3.7 shows data [50, 52] for a variety of pure, unfilled polymers plotted as the char yield measured after flaming combustion in a fire calorimeter versus the char residue at 900 ± 100°C for the same material after anaerobic pyrolysis in a TGA at a heating rate of about 10 K/min.

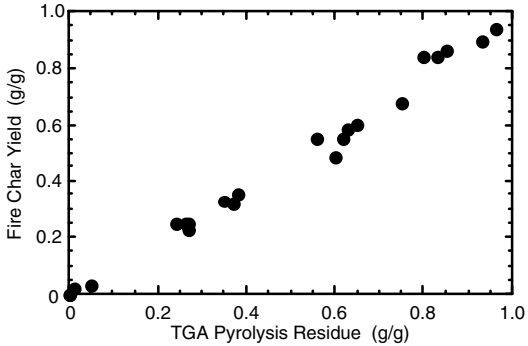

FIGURE 3.7 Char yield of plastics after burning versus anaerobic pyrolysis residue in TGA.

It is seen that the char yield of a material in a fire is essentially equal to its residual mass fraction after pyrolysis in an oxygen-free environment at temperatures representative of the char temperature in a fire. Although oxidative degradation products have been identified at the surface of noncharring olefinic polymers after flaming combustion, the data in Fig. 3.10 suggest that oxidation reactions in the solid during flaming combustion are not important to the overall fuel fraction as evidenced by the close agreement between fire char yield and anaerobic pyrolysis residue.

The phenomenological decomposition scheme above can be solved for the instantaneous fuel and char fractions in terms of the mass of polymer (P), intermediate (I^*), gas (G), and char (C) as follows. If k_i is the rate constant for initiation and k_r, k_g, and k_c are the rate constants for termination by recombination (k_r), hydrogen transfer to gaseous species (k_g), and cross-linking to char (k_c), respectively, then neglecting solid-state oxidation, the thermal decomposition reactions are [50, 52, 62]

$$P \underset{k_r}{\overset{k_i}{\rightleftharpoons}} I^* \qquad \text{(rapid equilibrium)} \tag{3.11}$$

$$I^* \xrightarrow{k_g} G \qquad \text{(slow)} \tag{3.12}$$

$$I^* \xrightarrow{k_c} C \qquad \text{(slow)} \tag{3.13}$$

and the system of rate equations for the species at time t is

$$\frac{dP}{dt} = -k_i P + k_r I^* \tag{3.14}$$

$$\frac{dI^*}{dt} = -k_i P - (k_r + k_g + k_c) I^* \tag{3.15}$$

$$\frac{dG}{dt} = k_g I^* \tag{3.16}$$

$$\frac{dC}{dt} = k_c I^* \tag{3.17}$$

According to the stationary-state hypothesis, $dI^*/dt \approx 0$, so that Eq. (3.15) provides the useful result

$$I^* = \left[\frac{k_i}{k_r + k_g + k_c}\right] P = KP$$

where $K = k_i/(k_r + k_g + k_c)$ is the pseudo-equilibrium constant for the polymer dissociation reaction. As the ratio of initiation to termination rate constants, K represents the kinetic chain length for degradation by depolymerization. Substituting $I^* = KP$ into Eqs. (3.14), (3.16), and (3.17),

$$\frac{dP}{dt} = -[k_i - Kk_r]P \tag{3.18}$$

$$\frac{dG}{dt} = k_g KP \tag{3.19}$$

$$\frac{dC}{dt} = k_c KP \tag{3.20}$$

With $I^* << P, G, C$, the total mass balance in terms of the initial mass m_o is

$$m_O = P + G + C + I^* \approx P + G + C \tag{3.21}$$

From Eqs. (3.18) to (3.21) with $dm_o/dt = 0$

$$\frac{dP}{dt} = -\frac{dC}{dt} - \frac{dG}{dt} = -[k_i - Kk_r]P \tag{3.22}$$

The sensible mass of the sample as measured, for example, in a TGA or fire calorimeter test is

$$m = P + C + I^* \approx P + C$$

and with Eqs. (3.18) to (3.20)

$$\frac{dm}{dt} = \frac{dP}{dt} + \frac{dC}{dt} = -\frac{dG}{dt} = -Kk_g P \tag{3.23}$$

Eq. (3.22) can be solved immediately for P in the isothermal case with initial condition $P = P_o = m_0$ at $t = 0$,

$$P = m_O \exp(-[k_i - Kk_r]t) \tag{3.24}$$

Substituting the isothermal result for P into Eq. (3.23) and separating variables

$$\int_{m_O}^{m} dm' = -\int_0^t Kk_g m_O \exp(-k_p t)\, dt \tag{3.25}$$

where k_p in the exponential of the integrand on the right-hand side of Eq. (3.25) is the overall rate constant for pyrolysis and is assumed to have the Arrhenius form

$$k_p = k_i - Kk_r = K(k_g + k_c) = A \exp\left(-\frac{E_a}{RT}\right) \tag{3.26}$$

in terms of the global activation energy E_a and frequency factor A for pyrolysis. The isothermal solution of Eq. (3.25) is

$$\frac{m(t)}{m_O} = 1 - \left[\frac{k_g}{k_g + k_c}\right](1 - e^{-k_p t}) \tag{3.27a}$$

or

$$\frac{m(t)}{m_O} = Y_c(T) + [1 - Y_c(T)]e^{-k_p t} \tag{3.27b}$$

Eqs. (3.27a) and (3.27b) show that the mass fraction $m(t)/m_0$ decreases exponentially with time and approaches an equilibrium value at a particular temperature as $t \to \infty$

$$Y_c(T) = \frac{m(\infty)}{m_O} = \frac{k_c}{k_g + k_c} \tag{3.28}$$

where $Y_c(T)$ is the equilibrium residual mass fraction or char yield at temperature T in terms of the rate constants for gas and char formation. Eq. (3.28) predicts a finite char yield at infinite time if $k_c > 0$ and zero char if $k_c = 0$.

The physical significance of a temperature-dependent, equilibrium char yield as the ratio of rate constants for gas and char formation is consistent with the use of group contributions for the

char-forming tendency of polymers developed by Van Krevelen [30, 46] (see the following section). If k_g and k_c have Arrhenius forms, Eq. (3.28) can be written

$$Y_c(T) = \left[1 + \frac{A_g}{A_c}\exp[-(E_g - E_c)/RT]\right]^{-1} \tag{3.29}$$

where E_c, E_g and A_c, A_g are the activation energies and frequency factors for char and gas formation, respectively. The crossover temperature T_{cr} is defined as the temperature at which the rates of gasification and cross-linking are equal, i.e., when $k_g = k_c$,

$$T_{cr} = \frac{(E_g - E_c)}{R\ \ln[A_g/A_c]} \tag{3.30}$$

It follows from Eq. (3.30) that the crossover condition, $k_g = k_c$, corresponds to the equilibrium residual mass fraction, $Y_c(T_{cr}) = 0.50$. If $Y_c(T)$ is the char yield at a temperature above the major mass loss transition temperature or the char yield is independent of temperature (e.g., an inert filler), then $Y_c(T) = \mu$ = constant and Eq. (3.27) is the solution for the isothermal mass loss history of a filled polymer with a nonvolatile mass fraction μ satisfying the rate law

$$\frac{dm}{dt} = -k_p(m - \mu m_O) \tag{3.31}$$

although Eq. (3.31) was not assumed a priori in the present derivation.

Charring. Char is the carbonaceous solid that remains after flaming combustion of the polymer. The char yield is the mass fraction of char based on the original weight of material. Charring competes with the termination reactions that generate volatile species and so reduces the amount of fuel in a fire. In addition, char acts as a heat and mass transfer barrier that lowers the flaming heat release rate. Fig. 3.7 demonstrated that the char yield in a fire is roughly equal to the anaerobic pyrolysis residue at high (flame) temperatures. Thus, char formation takes place in the solid state where oxidation reactions are slow compared to polymer dissociation and gas/char formation. The equivalence between the char yield and pyrolysis residue of a material permits a molecular interpretation of this important material fire parameter using the large volume of published thermogravimetric data and its correlation with chemical structure [30, 46].

Pyrolysis/char residue has the character of a thermodynamic quantity because it depends only on temperature and the composition of the material through the enthalpy barriers to gas and char formation, E_g, E_c, in Eq. (3.29). More precisely, char yield is a statistical thermodynamic concept wherein the total free energy of the char system at a particular (reference) temperature is the sum of the individual group contributions. Van Krevelen [30, 46] has devised a method for calculating the pyrolysis residue ($\approx$ char yield) of a polymer from its chemical composition and the observation that the char-forming tendency of different groups is additive and roughly proportional to the aromatic (i.e., nonhydrogen) character of the group. The char yield is calculated by summing the char-forming tendency per mole of carbon of the chemical groups, $C_{FT,i}$ and dividing by the molecular weight of the repeat unit

$$Y_c = \frac{C_{FT}}{M} \times M_{\text{carbon}} \times 100 = \frac{\sum_{1=1}^{N} n_i C_{FT,i}}{\sum_{1=1}^{N} n_i M_i} \times 1200 \tag{3.32}$$

The $C_{FT,i}$ is the amount of char per structural unit measured at 850°C divided by 12 (the atomic weight of carbon), i.e., the statistical amount of carbon equivalents in the char per structural unit of polymer. Negative corrections are made for aliphatic groups containing hydrogen atoms in proximity to char-forming groups because of the possibility for disproportionation and subsequent volatilization of chain-terminated fragments that are no longer capable of cross-linking. The method is empirical and relatively simple to use and good agreement is obtained with the measured pyroly-

sis residues (see Table 3.7). The char yield of polymers under anaerobic conditions is thus well described using the additive molar contributions of the individual groups comprising the polymer.

Kinetic Heat Release Rate. The previous results apply to the isothermal (constant temperature) case but processes of interest in fire and flammability are nonisothermal, e.g., thermogravimetric analyses at constant heating rate or fuel generation in the pyrolysis zone of a burning polymer. To calculate the instantaneous mass fraction $m(t)/m_0$ during a constant heating rate experiment where dT/dt = constant = β, begin by eliminating P between Eqs. (3.29) and (3.31) and integrating

$$\int_{m_0}^{m} dm' = (1 - Y_c)\int_{P_0}^{P} dP' \tag{3.33}$$

or since $P_o = m_o$,

$$\frac{m(T)}{m_O} = Y_c(T) + [1 - Y_c(T)]\frac{P(T)}{P_O} \tag{3.34}$$

For nonisothermal conditions $P(T)/P_o$ in Eq. (3.34) is obtained from Eq. (3.22)

$$\int_{P_O}^{P}\frac{dP'}{P'} = -\int_0^t k_p dt' = -\frac{A}{\beta}\int_{T_O}^{T}\exp\left(-\frac{E_a}{RT}\right)dT' \tag{3.35}$$

where the constant heating rate $\beta = dT/dt$ transforms the variable of integration from time t to temperature T, and A and E_a are the global frequency factor and activation energy of pyrolysis, respectively.

The right-hand side of Eq. (3.35) is the exponential integral, which has no closed-form solution. However, a good (± 2 percent) approximation for the exponential integral over the range of activation energies and temperatures encountered in thermal analysis and combustion is [64]

$$-\frac{A}{\beta}\int_{T_O}^{T}\exp\left(-\frac{E_a}{RT}\right)dT' \approx \frac{-ART^2}{\beta(E_a + 2RT)}\exp\left(-\frac{E_a}{RT}\right) = \frac{-k_p RT^2}{\beta(E_a + 2RT)} \tag{3.36}$$

Defining

$$y = \frac{k_p RT^2}{\beta(E_a + 2RT)} \tag{3.37}$$

the solution of Eq. (3.35) takes the form

$$\frac{P(T)}{P_O} = e^{-y} \tag{3.38}$$

Substituting Eq. (3.38) into Eq. (3.34), the residual mass fraction in a constant heating rate experiment is

$$\frac{m(T)}{m_O} = Y_c(T) + [1 - Y_c(T)]e^{-y} \tag{3.39}$$

which is the same form as the isothermal solution Eq. (3.27). Eqs. (3.37) and (3.39) show that the mass fraction is a function only of temperature and heating rate for a given set of material properties. Eq. (3.39) provides a good fit to data for residual mass fraction versus temperature [50, 52] such as that shown in Fig. 3.8A for PMMA and PAI. The fractional mass loss rate during a linear temperature ramp is obtained by differentiating Eq. (3.39) with respect to time,

$$\begin{aligned}\frac{-1}{m_O}\frac{dm(T)}{dt} &= (1 - Y_c(T))\frac{de^{-y}}{dt} + (1 - e^{-y})\frac{dY_c(T)}{dt} \\ &= (1 - Y_c(T))k_p(T)e^{-y} + \beta Y_c(T)(1 - Y_c(T))\frac{E_g - E_c}{RT^2}(1 - e^{-y})\end{aligned} \tag{3.40}$$

Because the rate of change of $Y_c(T)$ is small compared to the fractional mass loss rate at pyrolysis [50, 52], a good approximation is $Y_c(T) = \mu$ = constant so that $dY_c/dt = 0$ and Eq. (3.40) simplifies to

$$\frac{-1}{m_O}\frac{dm(T)}{dt} = (1 - \mu)k_p e^{-y} \tag{3.41}$$

Eq. (3.41) describes the fractional mass loss rate versus temperature at constant heating rate such as that shown in Fig. 3.8B for PMMA and PAI. The maximum value of the fractional mass loss rate (e.g., the peak heights in Fig. 3.8B) can be found by differentiating Eq. (3.41) with respect to time and setting this second derivative of the residual mass fraction equal to zero,

$$-\frac{d^2}{dt^2}\left(\frac{m(T)}{m_O}\right) = \beta(1-\mu)\frac{d}{dT}[k_p e^{-y}] = (1-\mu)k_p e^{-y}\left(\frac{\beta E_a}{RT^2} - k_p\right) = 0 \tag{3.42}$$

Eq. (3.42) has two roots: the trivial case $\mu = 1$ and

$$k_p(\max) = \frac{\beta E_a}{RT_p^2} \tag{3.43}$$

where T_p is the temperature at maximum mass loss rate during the course of the linear heating history. Fig. 3.8 shows TGA data at a constant heating rate of 10 K/min for two plastics of widely differing thermal stability: polymethylmethacrylate (PMMA) and polyamideimide (PAI). The onset of thermal degradation (mass loss) is seen as a knee in the mass fraction versus temperature curves (Fig. 3.8A). The onset degradation temperature T_d corresponds roughly to the temperature at which 5 percent of the pyrolyzable mass (initial mass minus char mass) is lost and values of $T_d = 350$ and 495 for PMMA and PAI, respectively, are shown in Fig. 3.8A. The residual mass at the end of the experiment is the pyrolysis residue. For pure polymers, the pyrolysis residue is the carbonaceous char fraction. For filled polymers, this pyrolysis residue will contain the inert filler in addition to the char (if any).

The time derivative of the mass fraction at each temperature in Fig. 3.8A is plotted in Fig. 3.8B. The temperature at the peak mass loss rate is T_p in Eq. (3.43) and this is seen to be 375° and 605°C for PMMA and PAI, respectively. The peak mass loss rate temperature corresponds roughly to the temperature at which 50 percent of the pyrolyzable mass is lost.

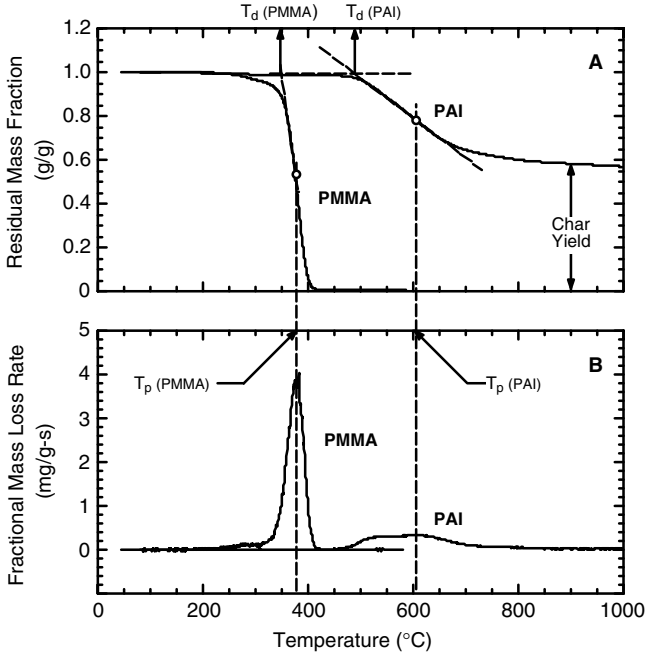

FIGURE 3.8 Residual mass fraction (A) and mass loss rate (B) of PMMA and PAI versus temperature at a heating rate of 10 K/min in nitrogen illustrating method used to obtain T_d and T_p from thermogravimetric data.

An analytic result for the peak fractional mass loss rate in a constant heating rate experiment is obtained by substituting Eq. (3.43) into Eq. (3.41)

$$\left.\frac{-1}{m_O}\frac{dm}{dt}\right|_{max} = (1-\mu)\frac{\beta E_a}{e^r RT_p^2} \tag{3.44}$$

where the exponent r of the natural number e in the denominator has the value

$$r = \left[1 + \frac{2RT_p}{E_a}\right]^{-1} \tag{3.45}$$

For the usual case where $E_a >> 2RT_p$ [58–62], Eq. (3.44) simplifies to

$$\left.\frac{-1}{m_O}\frac{dm}{dt}\right|_{max} \approx (1-\mu)\frac{\beta E_a}{eRT_p^2} \tag{3.46}$$

The temperature at peak mass loss rate T_p is obtained from the root E_a/RT_p of Eq. (3.49) written in the form

$$\ln\left[\frac{E_a}{RT_p}\right]^2 + \left[\frac{E_a}{RT_p}\right] + \ln\left[\frac{\beta R}{AE_a}\right] = 0 \tag{3.47}$$

Table 3.6 lists onset degradation temperatures (T_d) and maximum pyrolysis rate temperatures (T_p) for common plastics and elastomers obtained in a TGA at a heating rate of 10 K/min. The variability in decomposition temperatures of a plastic measured on different TGA instruments is about ±5°C. Real differences in decomposition temperatures for plastics from different sources are about ±10°C as seen by comparing PMMA decomposition temperatures in Fig. 3.8 and the average values T_d = 354 ± 8°C and T_p = 383 ± 9°C for eight samples of PMMA reported in Table 3.6. Also listed in Table 3.6 are the experimental values of the surface temperature at piloted ignition for the same [65–67] or similar [1–4, 68–71] plastics.

Eq. (3.47) shows that the peak mass loss temperature T_p increases with heating rate [50, 52]. There is general agreement [50, 52] between Eq. (3.44) and experimental data for plastics over a wide range of heating rates. By way of example, Eq. (3.44) predicts for PMMA with E_a = 160 kJ/mol [30], μ = 0, and T_p = 375°C (648 K) a peak mass loss rate at 10 K/min of (0.167 K/s)(160 kJ/mol)/($e^{0.94}$)(8.314 J/mol·K)(648 K)^2 ≈ 3 mg/g·s, which is in reasonable agreement with the value 3.7 mg/g·s in Fig. 3.8B.

The maximum specific heat release rate of the plastic is obtained by multiplying the peak kinetic mass loss rate [Eq. (3.46)] by the HOC of the pyrolysis gases. If h_c^o is the HOC of the pyrolysis gases, the maximum value of the specific heat release rate is [50, 72–74]

$$\dot{Q}_c^{max}(W/kg) = \left.\frac{-h_c^O}{m_O}\frac{dm}{dt}\right|_{max} = \frac{\beta h_c^O(1-\mu)E_a}{eRT_p^2} = \frac{\beta h_{c,s}^O E_a}{eRT_p^2} \tag{3.48}$$

where $h_{c,s}^o$ is the HOC of the pyrolysis gases per unit mass of original solid, which is related to the HOC of the polymer $h_{c,p}^o$ (see Table 3.3) and its char $h_{c,\mu}^o$ as

$$h_c^O = \frac{h_{c,p}^O - \mu h_{c,\mu}^O}{1-\mu} = \frac{h_{c,s}^O}{1-\mu} \tag{3.49}$$

Fig. 3.9 contains data for the specific heat release rate of plastics measured at a heating rate of 258 K/min (4.3 K/s) in a pyrolysis-combustion flow calorimeter [73, 74]. It is not immediately obvious that the specific heat release rate has any intrinsic value as a predictor of fire behavior, and much theoretical and experimental work is ongoing [72–74] to develop this relationship because of the ease of measuring specific heat release rate in the laboratory using small samples (milligrams) and the good correlation between this quantity and the ignition resistance and burning rate of plastics [50, 52, 72–74]. A rate-independent material flammability parameter emerges from this analysis when the maximum specific heat release rate Q_c^{max} (Ėq. (3.48)] is normalized for heating rate [72]

$$\eta_c = \frac{\dot{Q}_c^{max}}{\beta} = \frac{h_{c,s}^O E_a}{eRT_p^2} \tag{3.50}$$

TABLE 3.6 Decomposition and Ignition Temperatures of Plastics (Average Values ±10°C)

Polymer	ISO/ASTM Abbreviation	T_d °C	T_p °C	T_{ign} °C
Thermoplastics				
Acrylonitrile-butadiene-styrene	ABS	390	461	394
ABS FR	ABS-FR	—	—	420
Polybutadiene	BDR	388	401	378
Polyisobutylene (butyl rubber)	BR	340	395	330
Cellulose Acetate	CA	250	310	348
Cyanate Ester (typical)	CE	448	468	468
Polyethylene (chlorinated)	CPE	448	476	—
Polyvinylchloride (chlorinated)	CPVC	—	—	643
Polychloroprene rubber	CR	345	375	406
Polychlorotriuoroethylene	CTFE	364	405	580
Poly(ethylene-chlorotrifluoroethylene)	ECTFE	445	465	613
Phenoxy-A	EP	—	350	444
Epoxy (EP)	EP	427	462	427
Poly(ethylene-tetrafluoroethylene)	ETFE	400	520	540
Polyethylenevinylacetate	EVA	448	473	—
Fluorinated ethylene propylene	FEP	—	—	630
Poly(styrene-butadiene)	HIPS	327	430	413
Poly(styrene-butadiene) FR	HIPS-FR	—	—	380
Poly(p-phenyleneterephthalamide)	KEVLAR	474	527	—
Polyarylate (liquid crystalline)	LCP	514	529	—
Melamine formaldehyde	MF	350	375	350
Polyisoprene (natural rubber)	NR	301	352	297
Polytrifluoroethylene	P3FE	400	405	—
Polyamide 12	PA12	448	473	—
Polyamide 6	PA6	424	454	432
Polyamide 610	PA610	440	460	—
Polyamide 612	PA612	444	468	—
Polyamide 66	PA66	411	448	456
Polyamide 6 (glass reinforced)	PA6-G	434	472	390
Polyamideimide	PAI	485	605	526
Polyacrylamide	PAM	369	390	—
Polyacrylonitrile	PAN	293	296	460
Polyarylate (amorphous)	PAR	469	487	—
Polybutene	PB	—	390	—
Polybenzimidazole	PBI	584	618	—
Polybutylmethacrylate	PBMA	261	292	—
Polybenzobisoxazole	PBO	742	789	—
Polybutyleneterephthalate	PBT	382	407	382
Polybutyleneterephthalate	PBT-G	386	415	360
Polycarbonate	PC	476	550	500
Polycarbonate/ABS (70/30)	PC/ABS	421	475	440
Polycarbonate (glass reinforced)	PC-G	478	502	420
Polycaprolactone	PCL	392	411	—
Polyethylene (high density)	PE HD	411	469	380
Polyethylene (low density)	PE LD	399	453	377
Polyethylacrylate	PEA	373	404	—
Polyethylene-acrylic acid salt	PEAA	452	474	—
Polyetheretherketone	PEEK	570	600	570
Polyetherimide	PEI	527	555	528

TABLE 3.6 (*Continued*)

Polymer	ISO/ASTM Abbreviation	T_d °C	T_p °C	T_{ign} °C
	Thermoplastics			
Polyetherketone (e.g., KADEL)	PEK	528	590	—
Polyetherketoneketone	PEKK	569	596	—
Polyethylmethacrylate	PEMA	246	362	—
Polyethylenenaphthalate	PEN	455	495	479
Polyethyleneoxide	PEO	373	386	—
Polyethersulfone	PESU	533	572	502
Polyethyleneterephthalate	PET	392	426	407
Phenol formaldehyde	PF	256	329	429
Polytetrafluoroethylene-perfluoroether	PFA	—	578	—
Phenol formaldehyde	PF-G	—	—	580
Polymethylmethacrylate	PMMA	354	383	317
Poly(4-methyl-1-pentene)	PMP	—	377	—
Poly(α-methyl)styrene	PMS	298	333	—
Poly(α-methylstyrene)	PMS	250	314	—
Polyoxymethylene	POM	323	361	344
Polypropylene	PP	354	424	367
Polypropylene (isotactic)	PP (iso)	434	458	—
Polyphthalamide (AMODEL)	PPA	447	488	—
Polyphenyleneether	PPE	—	418	426
Poly(2,6-dimethylphenyleneoxide)	PPO	441	450	418
Polypropyleneoxide	PPOX	292	343	—
Polyphenylenesulfide	PPS	504	545	575
Polyphenylsulfone	PPSU	557	590	575
Polystyrene	PS	319	421	356
Polysulfone	PSU	481	545	510
Polytetrafluoroethylene	PTFE	543	587	630
Polytetramethyleneoxide	PTMO	—	352	—
PU (isocyanurate/rigid)	PU	271	422	378
Polyetherurethane rubber	PUR	324	417	356
Polyvinylacetate	PVAC	319	340	—
Polyvinylbutyral*	PVB	333	373	—
Polyvinylchloride (50% DOP)	PVC (ex)	249	307	318
Polyvinylchloride (rigid)	PVC (rigid)	273	285	395
Polyvinylchloride/polyvinylacetate blend	PVC/PVAC	255	275	—
Polyvinylidenechloride	PVDC	225	280	—
Polyvinylidenefluoride	PVDF	438	487	643
Polyvinylfluoride	PVF	361	435	476
Polyvinylcarbazole	PVK	356	426	—
Polyvinylalcohol	PVOH	298	322	—
Polyvinylpyridine	PVP	385	408	—
Polypara(benzoyl)phenylene	PX	476	602	—
Poly(styrene-acrylonitrile)	SAN	389	412	368
Phenylsilsesquioxane (silicone) resin	SI	475	541	—
Silicone rubber	SIR	456	644	407
Poly(stryene-maleic anhydride)	SMA	337	388	—
Polyimide thermoplastic	TPI	523	585	600
Polyurethane thermoplastic	TPU	314	337	271
Unsaturated polyester	UPT	330	375	380
Unsaturated polyester	UPT-G	—	—	395

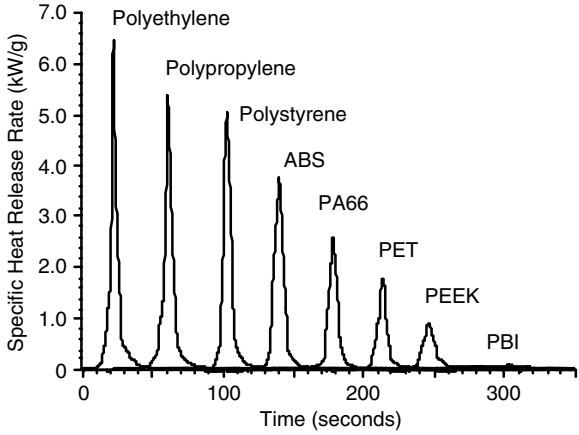

FIGURE 3.9 Specific heat release rate histories for some of the polymers in Table 3.7 (horizontally shifted for clarity). Dividing the maximum value (peak height) by the heating rate in the test ($\beta = 4.3$ K/s) gives the heat release capacity listed in Table 3.7.

The flammability parameter η_c has the units and significance of a heat [release] capacity (J/g·K) when the linear heating rate is β(K/s) and it contains only thermochemical properties of the material and the fundamental constants *e, R*. The heat release capacity η_c is a molecular-level flammability parameter that is the potential heat release per degree of temperature rise at the surface of a burning plastic. Table 3.7 contains ranked η_c values (± 10 percent) for commercial plastics and elastomers along with the measured HOC of the fuel gases $h_{c,s}^o$ and char yield μ [74].

TABLE 3.7 Heat Release Capacity, Heat of Combustion of Fuel Gases, and Char Yield of Plastics and Elastomers

Polymer	Abbreviation	HR capacity (J/g·K)	Total HR (kJ/g)	Char (%)
Polyethylene (low density)	PE LD	1676	41.6	0
Polypropylene	PP	1571	41.4	0
Epoxy (aliphatic amine cure)	EPA	1100	27	6
Polyisobutylene	BR	1002	44.4	0
Polystyrene	PS	927	38.8	0
Polystyrene (Isotactic)	PS (iso)	880	39.9	0
Polyhexamethylene sebacamide	PA610	878	35.7	0
Poly-2-vinylnaphthalene	PVN	834	39.0	0
Polyvinylbutyral	PVB	806	26.9	0.1
Polylaurolactam	PA12	743	33.2	0
Poly α-methylstyrene	PMS	730	35.5	0
Polyhexamethylene dodecanediamide	PA612	707	30.8	0
Acrylonitrile-butadiene-styrene	ABS	669	36.6	0
Phenoxy-A	EP	657	26.0	3.9
Polyethyleneoxide	PEO	652	21.6	1.7
Polyhexamethanyleneadipamide	PA66	615	27.4	0
Polyphthalamide	PPA	575	32.0	0
Polyphenyleneether	PPE	553	22.4	23
Polyvinylalcohol (>99%)	PVOH	533	21.6	3.3
Polcaprolactone	PCL	526	24.4	0

TABLE 3.7 (*Continued*)

Polymer	Abbreviation	HR capacity (J/g·K)	Total HR (kJ/g)	Char (%)
Polymethylmethacrylate	PMMA	514	24.3	0
Dicyclopentadienyl bisphenol cyanate ester	CED	493	20.1	27.1
Polycaprolactam	PA6	487	28.7	0
Polybutyleneterephthalate	PBT	474	20.3	1.5
Polyethylmethacrylate	PEMA	470	26.4	0
Polymethylmethacrylate	PMMA	461	23.2	0
Polyepichlorohydrin	ECR	443	13.4	4.8
Poly-n-butylmethacrylate	PBMA (n)	412	31.5	0
Poly-2,6-dimethyl-1,4-phenyleneoxide	PPO	409	20.0	25.5
Polyisobutylmethacrylate	PBMA (iso)	406	31.3	0
Polyethylmethacrylate	PEMA	380	26.8	0
Polyarylate	PAR	360	18.0	27
Polycarbonate of bisphenol-A	PC	359	16.3	21.7
Polysulfone of bisphenol-A	PSU	345	19.4	28.1
Polyethyleneterephthalate	PET	332	15.3	5.1
Bisphenol E cyanate ester	CEE	316	14.7	41.9
Polyvinylacetate	PVAC	313	19.2	1.2
Polyvinylidenefluoride	PVDF	311	9.7	7
Polyethylenenaphthylate	PEN	309	16.8	18.2
Poly(p-phenyleneterephthalamide)	KEVLAR	302	14.8	36.1
Bisphenol A cyanate ester	CEA	283	17.6	36.3
Tetramethylbisphenol F cyanate ester	CET	280	17.4	35.4
Poly(styrene-maleicanhydride)	SMAH	279	23.3	2.2
Epoxy novolac/Phenoxy-N	EPN	246	18.9	15.9
Polynorbornene	PN	240	21.3	6
Bisphenol-M cyanate ester	CEM	239	22.5	26.4
Polyethylenetetrafluoroethylene	ETFE	198	10.8	0
Polychloroprene	CR	188	16.1	12.9
Polyoxymethylene	POM	169	14.0	0
Polyacrylic Acid	PAA	165	12.5	6.1
Poly-1,4-phenylenesulfide	PPS	165	17.1	41.6
Liquid crystalline polyarylate	LCP	164	11.1	40.6
Polyetheretherketone	PEEK	155	12.4	46.5
Polyphenylsulphone	PPSU	153	11.3	38.4
Polyvinylchloride	PVC (rigid)	138	11.3	15.3
Polyetherketone	PEK	124	10.8	52.9
Novolac cyanate ester	CEN	122	9.9	51.9
Polyetherimide	PEI	121	11.8	49.2
Poly-1,4-phenyleneethersulfone	PESU	115	11.2	29.3
Polyacrylamide	PAK	104	13.3	8.3
Polyetherketoneketone	PEKK	96	8.7	60.7
Phenylsilsequioxane resin (toughened)	SI	77	11.7	73.1
Poly(m-phenylene isophthalamide)	NOMEX	52	11.7	48.4
Poly-p-phenylenebenzobisoxazole	PBO	42	5.4	69.5
LaRC-1A polyimide	PI	38	6.7	57
Polybenzimidazole	PBI	36	8.6	67.5
Polytetrafluoroethylene	PTFE	35	3.7	0
Polyamideimide	PAI	33	7.1	53.6
Hexafluorobisphenol-A cyanate ester	CEF	32	2.3	55.2
Thermoplastic polyimide	TPI	25	6.6	51.9
LaRC-CP2 polyimide	PI	14	3.4	57
LaRC-CP1 polyimide	PI	13	2.9	52

3.4 FIRE BEHAVIOR OF PLASTICS

The continuum-level treatment of the fire behavior of plastics that follows disregards the discrete (molecular) structure of matter so that the temperature distribution and, more importantly, its derivatives, are continuous throughout the material. In addition, the material is assumed to have identical thermal properties at all points (homogeneous) and in all directions (isotropic). The concept of a continuous medium allows fluxes to be defined at a point, e.g., a surface in one-dimensional space. Chemical reactions in the solid (pyrolysis) and flame (combustion) are assumed to occur so rapidly that the burning rate is determined solely by the heat transfer rate. Differential [75–78] and integral [79, 80] condensed-phase burning models have been developed from the continuum perspective with coupled heat and mass transfer for both charring and noncharring polymers. All of these models must be solved numerically for the transient (time-dependent) mass loss and heat release rates.

In the following simplified treatment of ignition and burning, the material response of a semi-infinite solid is assumed to be amenable to analysis by unsteady and steady heat transfer, respectively, at a constant surface heat flux. These simplified energy balances allow for the development of algebraic (scaling) relationships between the thermal properties of a plastic and its fire response, but ignore many important details such as transient behavior (see Fig. 3.13) that can only be captured through detailed numerical analyses.

3.4.1 Ignition

Ignition of plastics is a complicated phenomenon because the finite-rate solid-state thermochemistry (pyrolysis) is coupled to the gas phase chemistry (combustion) through the heat feedback from the flame (see Fig. 3.6). Ignition criteria for liquids and gaseous fuel/air mixtures are well established [3, 18–20, 81] because only the thermodynamic (equilibrium) state of the system need be considered. In particular, the reaction of gaseous fuels with air will be self-sustaining if the volumetric energy (heat) release of the equilibrium mixture is above a minimum (critical) value [81]. Sustained ignition of liquids and solids is complicated by the fact that there is dynamic coupling between the gas phase combustion and condensed-phase fuel-generating reactions because energy must be supplied to raise the temperature of the condensed phase to the fire point [3, 82] to generate combustible gases. The coupled, time-dependent nature of condensed-phase flaming combustion gives rise to a variety of proposed criteria for piloted ignition of solids [3, 82–84], but these can be roughly divided into thermal (solid state) and chemical (gas phase) criteria. Examples of thermal criteria for piloted ignition are a critical radiant heat flux and an ignition temperature. A piloted ignition temperature corresponds to a temperature at which the solid plastic decomposes to volatile fuel at a rate sufficient to maintain a flammable mixture at the igniter. Fig. 3.10 is a plot of ignition temperature versus gasification temperature of liquid and solid fuels. Plotted in Fig. 3.10 on the vertical axis are the piloted ignition and fire point temperatures of liquid and solid [1–4, 65–71] fuels, respectively, versus the mean thermal decomposition temperature of plastics [$(T_d + T_p)/2$ from Table 3.6], and the open cup flash point temperature of liquid hydrocarbons [81]. It is seen that the thermal decomposition temperature of plastics measured in laboratory thermogravimetric analysis at heating rates in the vicinity of 10 K/min give reasonable predictions of piloted ignition temperatures in standard ignition tests [85] and surface temperature measurements at piloted ignition [65–71].

Eq. (3.47) and experimental data [50] show that the decomposition temperature of polymers increases with heating rate, and there is some evidence that surface temperatures at ignition show a corresponding increase with radiant heating intensity [50]. Fig. 3.11 is a plot of measured surface temperatures at piloted ignition [67, 68] over a range of external heat fluxes for various plastics showing that the effect is small for these plastics over this range of heat flux.

Chemical criteria for solid ignition include a boundary layer reaction rate [82] and a critical pyrolyzate mass flux [3, 84], both of which are equivalent to establishing a lower flammability limit at the ignition source for a fixed test geometry and ventilation rate. Table 3.8 shows mass fluxes measured at ignition [67] and extinction [71, 88] for a number of plastics. Also listed are the effective HOCs h_c^{eff} EHOC of the fuel gases and the product of the mass flux and EHOC at ignition. It is seen that the heat release rate at ignition/extinction is relatively independent of the type of plastic.

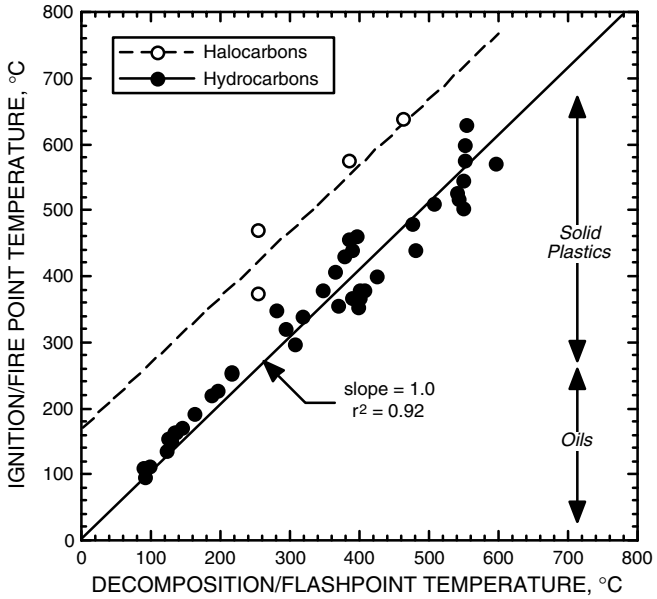

FIGURE 3.10 Ignition/fire point temperature versus decomposition/flash point temperature for solids/liquids.

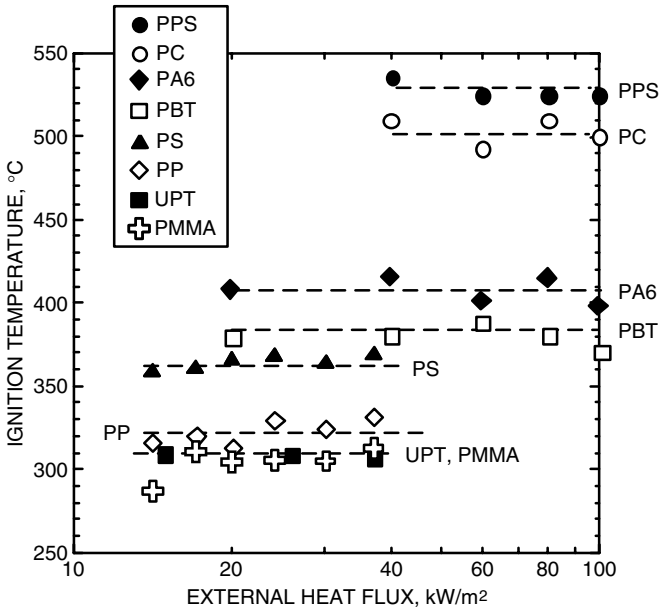

FIGURE 3.11 Ignition temperature versus external heat flux for PPS, PC, PA6, PBT [67], as well as PP, UPT, and PMMA [68].

TABLE 3.8 Effective Heat of Combustion (EHOC), Mass Loss Rate (MLR), and Heat Release Rate (HRR) of Polymers at Incipient Burning (Extinction and Ignition)

Material	HOC kJ/g	MLR g/m^2-s	HRR kW/m^2
	At extinction		
POM	14.4	4.5	65
PMMA	24.0	3.2	77
PE	38.4	2.5	96
CPE	13.6	7.0	95
PP	38.5	2.7	104
PS	27.0	4.0	108
PUR (foam)	17.4	5.9	101
PU (foam)	13.2	7.7	102
Extinction average:		4.7 ± 2.0	94 ± 15
	At ignition		
PMMA	24.8	4.4	109
EP	20.4	4.4	90
PA6	29.8	3.0	89
PBT	21.7	3.4	74
PC	21.2	3.4	72
PPS	23.5	3.6	85
PEN	22.9	2.7	62
PPA	24.2	3.1	75
PEEK	21.3	3.3	70
PESU	22.4	3.7	83
PPSU	23.8	4.3	102
Ignition average:		3.6 ± 0.6	83 ± 14

Thus, a chemical criterion is probably sufficient for ignition to occur but a critical surface temperature near the thermal decomposition temperature (see Table 3.6) is necessary to begin the fuel-generation process. Prior to ignition, the temperature history of a semi-infinite thickness of solid plastic is described by the one-dimensional energy equation for unsteady heat conduction with no internal heat generation and constant κ

$$\rho c \frac{\partial T}{\partial t} - \rho c v \frac{\partial T}{\partial x} = \kappa \frac{\partial^2 T}{\partial x^2} \tag{3.51}$$

where T is the temperature at location x in the solid polymer and $\alpha = \kappa/\rho c$ is the polymer thermal diffusivity in terms of its thermal conductivity κ, density ρ, and heat capacity c (see Table 3.2); v is the regression velocity of the burning surface. During the preheat phase prior to ignition, there is no surface regression, so $v = 0$ and Eq. (3.51) reduces to

$$\frac{\partial^2 T}{\partial x^2} - \frac{1}{\alpha} \frac{\partial T}{\partial t} = 0 \tag{3.52}$$

The solution of Eq. (3.52) for the ignition time t_{ign} of a thermally thick sample with constant α and net heat flux $\dot{q}_{net}$ at the surface $x = 0$ is [89]

$$t_{ign} = \frac{\pi}{4} \kappa \rho c \left[\frac{T_{ign} - T_O}{q_{net}} \right]^2 \tag{3.53}$$

where T_{ign} is the (piloted) ignition temperature and T_o is the ambient initial temperature. If the sample thickness b is less than a millimeter or so, ignition occurs at time

$$t_{ign} = \rho bc\left[\frac{T_{ign} - T_O}{q_{net}}\right] \tag{3.54}$$

Eqs. (3.53) and (3.54) define a time to ignition that is determined by the net heat flux and the ignition (decomposition) temperature, sample thickness, and thermal and transport properties of the material κ, ρ, c. The net heat flux at the surface, $\dot{q}_{net} = \dot{q}_{ext} - \dot{q}_{rerad} - \dot{q}_{conv} - \dot{q}_{cond}$ is the heat influx from an external source $\dot{q}_{ext}$ minus the heat losses by reradiation $\dot{q}_{rerad}$ and convection $\dot{q}_{conv}$ to the cooler environment, and conduction into the solid $\dot{q}_{cond}$, respectively. For high heat fluxes and/or thermally thick samples, substituting the net heat flux at incipient (pre)ignition into Eq. (3.53) and rearranging gives

$$\frac{1}{\sqrt{t_{ign}}} = \frac{\dot{q}_{ext} - \dot{q}_{crit}}{TRP} = \frac{\dot{q}_{ext} - CHF}{TRP} \tag{3.55}$$

where

$$TRP = \sqrt{\pi\kappa\rho c/4}(T_{ign} - T_\infty) \tag{3.56}$$

is a quantity known as the thermal response parameter (TRP) [88, 90] and

$$CHF = \dot{q}_{rerad} + \dot{q}_{conv} + \dot{q}_{cond} \cong \sigma(T_{ign}^4 - T_0^4) + h(T_{ign} - T_0) \tag{3.57}$$

is the critical heat flux for ignition. Eq. (3.55) suggests that CHF can be obtained experimentally as the $\dot{q}_{ext}$ intercept at $1/\sqrt{t_{ign}} = 0$ from a linear plot of $1/\sqrt{t_{ign}}$ versus external heat flux. However, the assumption of a semi-infinite solid breaks down at the long times/low heat fluxes near the critical condition when the sample temperature approaches the surface temperature and Eq. (3.53) no longer applies. Critical heat fluxes are best obtained by bracketing procedures and/or by measuring the external heat flux at which the flame spread rate asymptotically approaches zero in a gradient heat flux experiment [91]. Fig. 3.12 shows experimental data [66] for time to ignition at various heat fluxes for polycarbonate (PC) and the graphical procedures used to obtain TRP and CHF. Table 3.9 is a listing of TRPs reported for these plastics or calculated from heat flux and time-to-ignition data [65–71, 90–108], averaged for multiple values, along with the measured and calculated CHF. Calculated values of CHF were obtained from Eq. (3.57) with $h = 15$ W/m^2(K [91, 92] with $T_{ign} = (T_d + T_p)/2$. The agreement between measured and calculated CHF is within the variation in CHF from different sources.

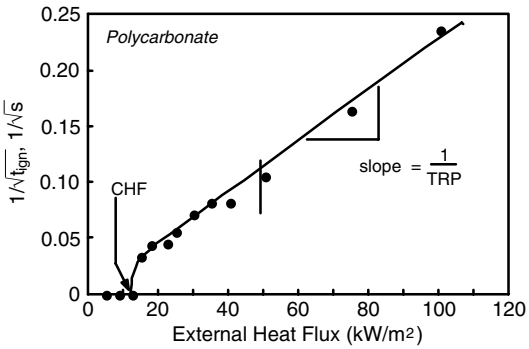

FIGURE 3.12 Reciprocal square root of time to ignition versus external heat flux for polycarbonate showing graphical method for determining CHF and TRP. (Data from Ref. 66.)

TABLE 3.9 Thermal Response Parameters (TRP) and Critical Heat Fluxes (CHF) for Ignition

Polymer	TRP $kW \cdot s^{1/2} m^{-2}$	Critical heat flux (CHF) kW/m^2 (Measured)	Critical heat flux (CHF) kW/m^2 (Calculated)
ABS	365	9–15	19
ABS FR	330	13	19
BR	211	19	16
CE (typical)	534	27	22
CPVC	591	40	—
CR	245	20–37	17
CTFE	460	30	16
ECTFE	410	38–74	43
EP	425	20	13
EP-G	462	10–15	13
ETFE	478	17–27	32
FEP	682	38–50	47
HIPS	420	—	15
HIPS-FR	351	—	15
LCP-G (30%)	—	32	30
LCP-M (45%)	—	22	30
MF	324	25	14
NBR	308	26	—
NR	294	17	11
P3FE	504	—	17
PA6	461	15–20	20
PA66	352	15–21	20
PA6-G (10%)	303	—	22
PA6-G (20%)	315	—	22
PA6-G (30%)	318	—	22
PA6-G (5%)	371	—	22
PAI	378	40–50	33
PBI	—	≈60	41
PBT	520	20	16
PBT-G (10%)	317	—	17
PBT-G (20%)	308	—	17
PBT-G (30%)	325	—	17
PBT-G (5%)	381	—	17
PC	455	15–20	29
PC/ABS	344	—	21
PC/ABS-FR	391	—	—
PC-G (10%)	383	—	26
PC-G (20%)	362	—	26
PC-G (30%)	373	—	26
PC-G (5%)	402	—	26
PE HD	343	15	21
PE LD	454	—	19
PE-XL	442	—	—
PE-XL/FR	581	—	—
PEEK	623	30–40	39
PEEK-G	301	—	—
PEI	435	25–40	32
PEN	545	24	24

TABLE 3.9 (*Continued*)

Polymer	TRP $kW \cdot s^{1/2} m^{-2}$	Critical heat flux (CHF) kW/m^2 (Measured)	Critical heat flux (CHF) kW/m^2 (Calculated)
PESU	360	19–30	34
PESU-G	258	—	—
PET	403	10–19	18
PF	537	15–26	9
PF-G	610	20	9
PFA	787	—	38
PMMA	274	6–23	12
POM	269	13	12
PP	193–336	15	21
PPA-G	—	29	23
PPA-G/FR	—	15	23
PPE	323	—	15
PP	415	15	16
PP-FR	310	10	—
PPO	342	19	16
PPS	395	35–38	37
PPS-G (5%)	450	—	37
PPS-G (10%)	468	—	37
PPS-G (20%)	490	—	37
PPS-G (30%)	466	—	37
PPSU	512	32–35	33
PS	355	6–13	10
PSU	424	26	24
PTFE	654	50	34
PUR	347	23	10
PVC (rigid)	410	15–28	7
PVC (flex)	174	21	9
PVDF	609	30–50	26
PVF	303	—	15
PX	626	—	28
SBR	198	10–15	—
SIR	429	34	23
TPI	—	36–50	32
UPT	343	—	10
UPT-G	483	10–15	12
UPT-M	752	—	—
VE	285	—	—
VE-G	443	—	—

Table 3.10 is a list of thermal inertia values. Values in the first column of Table 3.10 were calculated from Table 3.2 as the product of room temperature values, that is, $\kappa_0\rho_0 c_0$ (298 K) = $(\kappa\rho c)_0$. The second column lists the thermal inertia at ignition calculated as $\kappa\rho c = (\kappa\rho c)_0 T_{ign}/T_0$ according to Eq. (3.4). The last column in Table 3.10 lists experimental values for $\kappa\rho c$ extracted from the TRP in Table 3.9 using Eq. (3.56) and T_{ign} reported in Table 3.6. It is seen that the approximation $\kappa\rho c(T_{ign}) \approx (\kappa\rho c)_0 T_{ign}/T_0$ gives qualitative (±25 percent) agreement with experimental values.

TABLE 3.10 Thermal Inertia: Measured and Calculated (All Values in Units kW^2-s-m^{-4}-K^{-2})

Polymer	$k\rho c(T_0)$	$(k\rho c)_0 T_{ign}/T_0$	$k\rho c$ (Fire data)
ABS	0.41	0.92	1.1
EP	1.2	1.9	1.6
FEP	0.63	1.9	1.6
MF	0.52	1.1	1.3
EP	0.39	0.91	1.6
PPO	0.22	0.51	0.77
HIPS	0.31	0.73	1.5
PA6	0.42	1.0	1.4
PA66	0.41	1.0	0.50
PAI	0.34	0.91	0.72
BR	0.42	0.91	1.3
PBT	0.48	1.1	1.1
PC	0.29	0.76	0.96
CR	0.30	0.69	0.75
SIR	0.35	0.81	1.8
PET	0.59	1.3	1.4
PEEK	0.45	1.3	0.68
PEI	0.36	0.96	0.95
PESU	0.28	0.73	0.72
PUR	0.37	0.78	1.6
PE MD	0.63	1.3	1.4
ETFE	0.41	1.1	0.58
PE HD	0.82	1.8	3.9
PEAA	0.40	1.1	1.0
PEN	0.0	0.0	2.1
TPI	0.17	0.49	1.1
BR	0.23	0.47	0.61
NR	0.20	0.38	1.5
PMMA	0.33	0.65	1.1
POM	0.45	0.93	0.90
PPE	0.30	0.71	0.82
PPS	0.38	1.1	0.55
PPO	0.29	0.68	0.77
PPSU	0.24	0.68	0.68
PP	0.25	0.53	0.91
PS	0.18	0.39	0.74
PS-FRP	0.18	0.37	3.6
PSU	0.36	0.94	1.3
PTFE	0.56	1.7	0.85
PVC	0.26	0.59	0.35
PVF	0.25	0.63	0.51
SI	0.67	1.5	1.6
SBR	0.35	0.78	0.58
UPT	0.73	1.6	2.2

3.4.2 Steady Burning

Once sustainable ignition has occurred, steady, one-dimensional burning of the polymer is assumed. Steady burning at a constant surface heat flux is treated as a stationary state by choosing a coordinate system that is fixed to the surface and moving at the recession velocity v. If there is no internal

heat generation or absorption, the one-dimensional heat conduction equation [Eq. (3.51)] applies. Because semicrystalline polymers absorb the heat of fusion during melting at temperatures below the decomposition temperature, Eq. (3.51) is only approximate for these materials. Under steady-state conditions, $dT(x)/dt = 0$ so that Eq. (3.51) becomes, for steady burning [50, 52]

$$\frac{d^2T}{dx^2} + \frac{v}{\alpha}\frac{dT}{dx} = 0 \tag{3.58}$$

The general solution of Eq. (3.58) for a material with constant thermal diffusivity is

$$T(x) = c_1 + c_2\exp[-vx/\alpha] \tag{3.59}$$

Two boundary conditions are needed to evaluate the constants of integration c_1 and c_2 in Eq. (3.59). Conservation of energy at the pyrolysis front $x = 0$ gives

$$\kappa\frac{dT(x)}{dx}\bigg|_{x=0} = -\dot{q}_{\text{net}} + \rho v\Delta h_v = -c_2\frac{\kappa v}{\alpha} \tag{3.60}$$

from which $c_2 = (\alpha/\kappa v) - (\Delta h_v/c)$ with Δh_v the latent heat of vaporization of the pyrolysis products and the net heat flux at the surface ($x = 0$)

$$\begin{aligned}\dot{q}_{\text{net}} &= \dot{q}_{\text{ext}} + \dot{q}_{\text{flame}} - \dot{q}_{\text{rerad}} - \dot{q}_{\text{cond}} \\ &= \dot{q}_{\text{ext}} + \dot{q}_{\text{flame}} - \dot{q}_{\text{loss}}\end{aligned} \tag{3.61}$$

Eq. (3.61) defines the net heat flux into the surface under conditions of flaming combustion $\dot{q}_{\text{net}}$ as the difference between the heat flux entering the surface from an external radiant energy source $\dot{q}_{\text{ext}}$ and/or surface flame $\dot{q}_{\text{flame}}$, and the heat losses $\dot{q}_{\text{loss}}$ due to surface reradiation, convection, and conduction into the solid.

On the rear face of the semi-infinite slab ($x = \infty$) specify $dT/dx = 0$ or, equivalently, $T(\infty) = T_o = c_1$ where T_o is the backside (ambient) temperature. The final temperature distribution during steady-state burning of a semi-infinite thickness of combustible plastic is

$$T(x) = T_{\text{O}} + \left[\frac{\dot{q}_{\text{net}}}{\rho cv} - \frac{\Delta h_v}{c}\right]\exp\left[-\frac{v}{\alpha}x\right] \tag{3.62}$$

The steady burning velocity of the surface $x = 0$ at temperature $T(0) = T_p$ from Eq. (3.62) is

$$v = \frac{1}{\rho}\frac{\dot{q}_{\text{net}}}{(c(T_p - T_{\text{O}}) + \Delta h_v)} = \frac{1}{\rho}\frac{\dot{q}_{\text{net}}}{h_g} \tag{3.63}$$

where the total heat of gasification h_g per unit original mass of polymer is [see Eq. (3.6)],

$$h_g = (\Delta h_s + \Delta h_f + \Delta h_d) + \Delta h_v \approx c(T_p - T_{\text{O}}) + \Delta h_v. \tag{3.64}$$

Eqs. (3.62) and (3.63) allow the steady-state temperature distribution in the burning solid polymer to be expressed

$$T(x) - T_{\text{O}} = (T_p - T_{\text{O}})\exp\left(-\frac{c\,\dot{q}_{\text{net}}}{\kappa\,h_g}x\right)$$

which is in general agreement with experimental data for the temperature gradient in steadily gasifying PMMA slabs [50].

Conservation of mass for a virgin polymer of density ρ that pyrolyzes to an inert fraction or char residue μ gives [50, 52]

$$\rho v = \frac{\dot{m}_g}{1 - \mu} \tag{3.65}$$

where $\dot{m}_g$ is the mass loss rate of pyrolysis gases per unit surface area. Defining a heat of gasification per unit mass of volatiles [Eq. (3.8)]

$$L_g = \frac{h_g}{1 - \mu}$$

and combining Eqs. (3.8) and (3.65)

$$\dot{m}_g = \frac{\dot{q}_{\text{net}}}{h_g/(1 - \mu)} = \frac{\dot{q}_{\text{net}}}{L_g} \tag{3.66}$$

shows that the heat of gasification per unit mass of solid polymer h_g can be determined from the reciprocal slope of a plot of areal mass loss rate versus external heat flux if the char yield is measured after the test, since from Eqs. (3.61) and (3.66)

$$\dot{m}_g = \frac{\dot{q}_{\text{ext}}}{L_g} - \left(\frac{\dot{q}_{\text{flame}} - \dot{q}_{\text{loss}}}{L_g} \right) \tag{3.67}$$

Multiplying Eq. (3.67) by the net heat of complete combustion of the volatile polymer decomposition products h_c^o and the gas phase combustion efficiency χ gives the usual result for the average heat release rate of a burning specimen [3, 71].

$$\dot{q}_c = \chi h_c^0 \dot{m}_g = \chi(1 - \mu) \frac{h_c^0}{h_g} \dot{q}_{\text{net}} = \text{HRP } \dot{q}_{\text{net}} \tag{3.68}$$

The dimensionless material sensitivity to external heat flux in Eq. (3.68)

$$\text{HRP} = \chi(1 - \mu) \frac{h_c^0}{h_g} = \chi \frac{h_c^0}{L_g} \tag{3.69}$$

is called the heat release parameter [102]. Fire calorimetry is used to obtain HRP as the slope of heat release rate versus external heat flux or as the ratio h_c^{eff}/L_g from individual measurements. Tewarson [71] has reported HRP values for many common polymers and composites and has used this fire parameter for predicting the fire propagation tendency and heat release rate of materials [90, 103, 104]. Table 3.11 lists values for HRP, the effective heat of flaming combustion HOC = χh_c^o, and the heat of gasification L_g for plastics, elastomers, flame-retarded (-FR) plastics, and fiberglass reinforced plastics (-G) as reported in or calculated from data in the literature [65–72, 88, 90, 91, 93–108].

Fig. 3.13 shows typical heat release rate histories for thermally thick and thin polymers that gasify completely or form a char during burning. It is apparent that none of these heat release rate histories shows a constant (steady-state) value of heat release rate over the burning interval as presumed in the derivation of Eq. (3.68). Thus, the interpretation of time-varying heat release rate histories in terms of Eq. (3.68) is a subject of active research [109, 110] that attempts to account for phase transitions (e.g., melting), time-varying temperature gradients, finite sample thickness, and char formation during burning. The left-hand curves in Fig. 3.13 are characteristic of noncharring ($\mu = 0$) plastics of different thicknesses. The heat release histories for the charring plastics on the

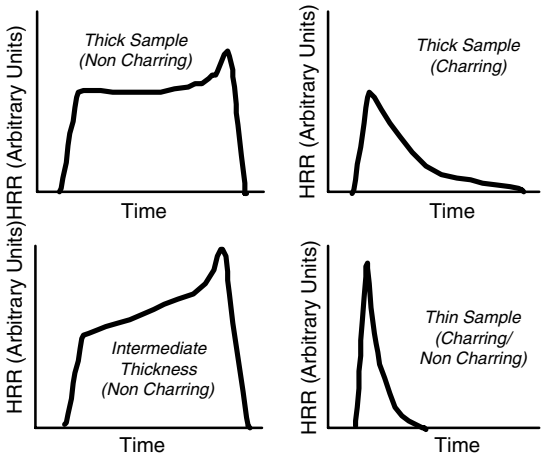

FIGURE 3.13 Typical heat release rate (HRR) histories for thick and thin samples of charring and noncharring plastic.

right-hand side of Fig. 3.13 show the typical peak in heat release rate soon after ignition followed by a depression in the heat release rate as the char layer increases in thickness. The growing char layer insulates the underlying plastic from the surface heat flux so that the net heat flux at the in-depth pyrolysis front decreases with time. Char can also act as a mass diffusion barrier to the volatile fuel. Charring polymers can be linear, branched, or cross-linked thermoplastics, elastomers, or thermosets having amorphous or semicrystalline morphologies.

In all cases the time integral (area under) the heat release rate history per unit mass of plastic consumed by burning is the effective heat of flaming combustion (EHOC). The EHOC is determined primarily by the combustion chemistry in the flame and the ventilation rate. Combustion efficiency decreases when halogens are present in the polymer molecule or gas phase active flame-retardant chemicals are added, when soot or smoke is produced in large yield, or when there is insufficient oxygen for complete conversion of the organic fuel to carbon dioxide and water. Flaming combustion efficiency appears to be relatively independent of the charring tendency of a polymer.

Fig. 3.14 shows fire calorimetry data for the average heat release rate of plastics versus their char yield after burning or pyrolysis. The linear dependence of heat release rate on char yield predicted by Eq. (3.68) is not observed in Fig. 3.14, indicating that char formation contributes more to flammability reduction than simply reducing the fuel fraction, e.g., acts as a barrier to the transfer of mass and heat during burning as illustrated schematically in Fig. 3.13.

Fig. 3.15 shows experimental heat release rate histories for 6-mm-thick samples of high-density polyethylene (ultra high molecular weight) at external heat fluxes of 35, 50, 65, and 80 kW/m^2. At no time during the heat release rate history of polyethylene is steady (time independent) burning observed. Fig. 3.16 is a plot of data for the peak heat release rate of PA6 versus external heat flux from two different sources [67, 99] showing typical variation. The slope of the linear fit of data in Fig. 3.16 is the heat release parameter HRP, and the intercept is the heat release rate at zero external heat flux HRR_0.

The significance of HRR_0 as a flammability parameter is seen by combining Eqs. (3.61) and (3.68) and separating the heat release rate into unforced and forced components

$$\dot{q}_c = \left[\left(\chi(1-\mu)\frac{h_c^0}{h_g}\right)(\dot{q}_{\text{flame}} - \dot{q}_{\text{loss}})\right] + \left[\chi(1-\mu)\frac{h_c^0}{h_g}\right]\dot{q}_{\text{ext}} \tag{3.70}$$

or

$$\dot{q}_c = \mathrm{HRR}_0 + \mathrm{HRP}\,\dot{q}_{\text{ext}} \tag{3.71}$$

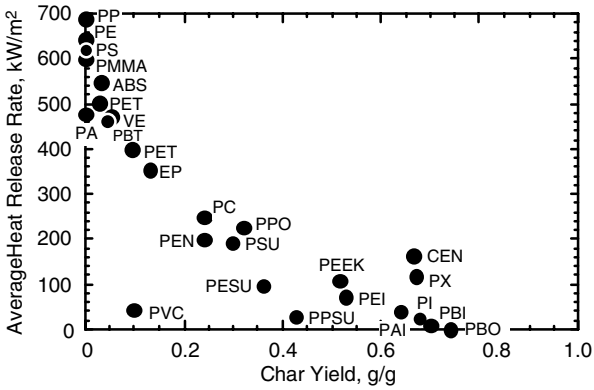

FIGURE 3.14 Average heat release rates versus pyrolysis residue/char yield of plastics.

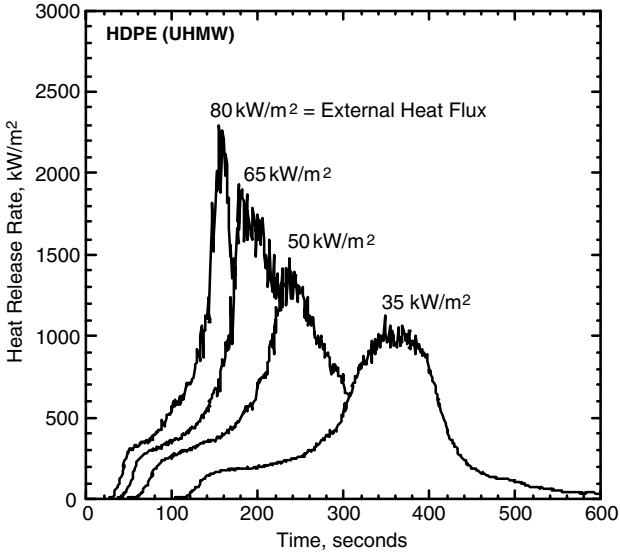

FIGURE 3.15 Heat release rate histories of polyethylene (high density/ultra high molecular weight) at 35, 50, 65, and 80 kW/m^2 external heat flux showing effect on time to ignition and peak/average heat release rates.

Eqs. (3.70) and (3.71) show that the heat release rate of the plastic is comprised of an intrinsic heat release rate HRR_0 in unforced flaming combustion and an extrinsic heat release rate HRP $\dot{q}_{ext}$ in forced flaming combustion. Because HRR_0 is primarily driven by the flame heat flux, it will be a function of the size and ventilation rate in the fire test and therefore is expected to be somewhat apparatus dependent and reflective of a particular combustion environment.

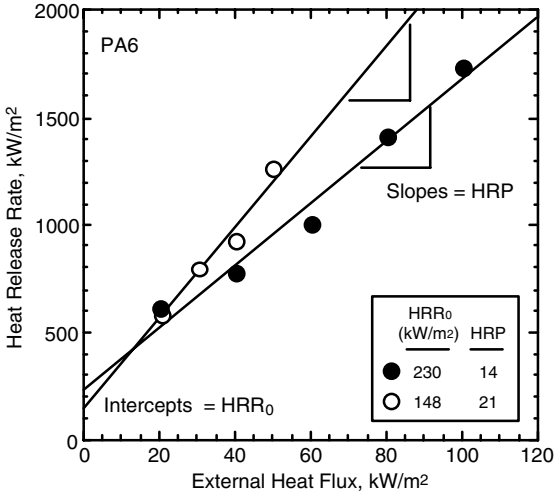

FIGURE 3.16 Peak heat release rate versus external heat flux for PA6 showing graphical procedure for determining HRP and HRR_0 as the slope and intercept, respectively. (Solid circles, Ref. 99; open circles, Ref. 67.)

The first term on the right-hand side of Eq. (3.71), HRR_0, has the units and significance of an ideal [101] or intrinsic [111] heat release rate of the material burning under ambient (unforced) conditions and has the functional form

$$HRR_0 = \left(\chi(1 - \mu)\frac{h_c^0}{h_g}\right)(\dot{q}_{flame} - \dot{q}_{loss}) = HRP(\dot{q}_{flame} - \dot{q}_{loss}) \tag{3.72}$$

Increasing the oxygen concentration in the combustion atmosphere increases the flame heat flux [112] and thus increases HRR_0 [107, 111], since HRP and $\dot{q}_{loss}$ depend primarily on the properties of the solid.

TABLE 3.11 Effective Heats of Combustion (EHOC), Heats of Gasification (L_g), and Heat Release Parameters (HRP) of Plastics and Elastomers

Plastic	EHOC, (MJ/kg)	L_g (MJ/kg)	HRP
ABS	29.0	2.3	13
ABS-FR	10.2	2.5	4
CEA	25.9	4.0	7
CEE	25.1	5.1	5
CEF	16.9	3.0	6
CEM	28.9	3.0	10
CEN	20.6	5.0	4
CET	25.9	3.5	7
CPE (25% Cl)	22.6	2.1	11
CPE (36% Cl)	10.6	2.8	4
CPE (48% Cl)	7.2	3.3	2
CPVC	3.9	2.0	2
CR	17.6	2.0	9
CTFE	6.5	0.7	9
ECTFE	4.6	1.5	3
EP	20.4	1.6	13
EPDM	29.2	1.9	15
EP-G	21.1	2.3	9
ETFE	7.3	1.1	6
EVA	30.8	—	—
FEP	1.3	1.5	2
HIPS	28.1	2.0	14
HIPS-FR	10.3	2.1	5
LCP	14.8	—	—
NR	30.2	2.0	15
PA6	29.8	1.5	20
PA66	28.2	2.1	18
PAI	19.3	4.8	4
PBI	22.0	5.5	4
PBT	21.7	1.4	16
PBT-FR	13.7	2.3	6
PC	21.2	2.4	9
PC/ABS	22.4	2.0	11
PC/ABS-FR	17.7	2.5	7
PC-FR	10.4	3.5	3
PE HD	40.3	2.2	18
PE LD	40.3	1.9	21
PEEK	21.3	3.4	6
PEEK-G	20.5	5.8	4

TABLE 3.11 (*Continued*)

Plastic	EHOC, (MJ/kg)	L_g (MJ/kg)	HRP
PEI	21.8	3.5	6
PEN	22.9	2.5	5
PESU	22.4	5.6	4
PESU-G	16.0	5.3	3
PET	18.0	1.4	13
PE-XL	31.4	6.3	5
PE-XL/FR	20.1	5.2	4
PF	16.3	5.4	3
PFA	2.2	0.9	2
PMMA	24.8	1.7	14
POM	14.4	2.4	6
PP	41.9	1.9	22
PPA	24.2	1.4	17
PPO/PS	22.9	1.5	15
PPO-G	25.4	8.5	3
PPS	23.5	6.3	4
PPSU	23.8	5.6	4
PS	27.9	1.8	16
PS-FR	13.8	2.0	7
PSU	20.4	2.5	8
PTFE	4.6	2.3	2
PU	16.3	3.3	5
PUR	24.0	1.3	18
PVC (flexible)	11.3	2.3	5
PVC (rigid)	9.3	2.7	3
PVC/PMMA	10.0	4.0	3
PVDF	3.8	1.9	2
PVF	4.1	1.0	4
PX	20.0	5.0	4
SBR	31.5	2.3	18
SIR	21.7	2.7	8
TPI	12.0	2.4	5
TPU	23.5	2.3	10
UPT	23.4	3.0	8
UPT-FR	15.0	4.2	4
VE	22.0	1.7	13

3.4.3 Unsteady Burning

The heat release rate in forced flaming combustion is the single best indicator of the fire hazard of a material in an enclosure [113], yet none of the tens of billions of pounds [114] of flame-retardant plastics sold worldwide each year in consumer electronics, electrical equipment, building and construction, home furnishings, automobiles, and public ground transportation are required to pass a heat release rate test. Instead, a flame test of ignition resistance [21] is the only fire hazard assessment required of these plastics [12]. Ignition resistance (flammability) tests rank materials according to the duration or extent of burning after removal of a small-flame (e.g., a bunsen burner) ignition source. The Underwriters Laboratory [21] test for flammability of plastics rates materials according to their tendency to burn at a particular rate in a horizontal configuration (UL 94 HB) or self-

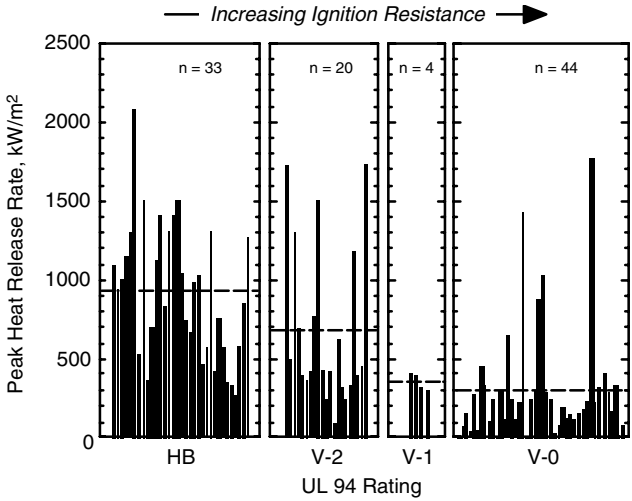

FIGURE 3.17 Peak heat release rates of 106 plastics at external heat flux of 50 ± 10 kW/m^2 grouped according to ignition resistance rating in the UL 94 test.

extinguish in a specified period of time (10 or 30 s) in a vertical orientation (UL 94 V-0/1/2) after being ignited from below by a bunsen burner. Another widely used flammability rating is the limiting oxygen index (LOI) [115], which is the oxygen concentration in a metered gas stream flowing past a thin (2 to 3 mm) downward-burning bar of material that results in flame extinguishment at 180 s. The tendency of a material to cease combustion or self-extinguish after removal of the ignition source is termed ignition resistance. Empirical correlation of bench-scale [116, 117] and full-scale [118–125] fire behavior with standardized [21, 115] ignition resistance (flammability) tests indicates a general trend of improved fire safety for flame-resistant and fire-retardant plastics [125]. However, a formal relationship between fire behavior and flammability, and between the flammability tests themselves, remains obscure.

Fig. 3.17 shows the peak heat release rates of 106 plastics, plastic blends, and composites measured at an external heat flux of 40, 50, or 60 kW/m^2 (typically 50 kW/m^2). Peak heat release rates are grouped according to their flammability rating in the Underwriters Laboratory test (UL 94) for flammability of plastics [21]. Average peak heat release rates for the n samples in each category are indicated by the horizontal dashed lines in Fig. 3.5, and these are 926 ± 427, 686 ± 513, 359 ± 54, and 294 ± 340 kW/m^2 for HB, V-2, V-1, and V-0 ratings, respectively. Although the average value of the peak heat release rate decreases as ignition resistance increases, the range and variation of heat release rates in Fig. 3.17 for any particular UL 94 rating precludes the use of a single heat release rate measurement as an indicator of flammability. More important in context of fire safety is the observation that ignition resistance is a poor predictor of fire hazard, i.e., heat release rate [113].

The poor agreement between heat release rate in forced flaming combustion and the self-extinguishing tendency of plastics in the absence of external heating can be understood by consideration of Eq. (3.70). After a solid combustible material is ignited and the ignition source is removed, flaming will cease if the rate of heat released by the burning sample is insufficient to drive the fuel generation (evaporation or pyrolysis) at a rate that will maintain a flammable mixture in the gas phase. As the lower limit of flammability of diffusion flames shows a strong dependence on the fuel composition and concentration [126], a critical mass flux criterion for persistent ignition of plastics would not be expected to broadly apply because the volatile fuel species (pyrolyzate) can vary significantly between polymers [51] so that the lower flammability limit would be material dependent.

Table 3.8 indicates that a critical value of the heat release rate is a better indicator of incipient burning (ignition or extinction). During the ignition phase of the UL 94 or limiting oxygen index test when the bunsen burner is in contact with the plastic specimen [Eq. (3.71)]

$$\mathrm{HRR}_0 + \mathrm{HRP}\,\dot{q}_{\mathrm{ext}} - \dot{q}_c = 0 \tag{3.73}$$

If a critical heat release criterion extends to these flammability tests and incipient burning satisfies

$$\mathrm{HRR}_0 + \mathrm{HRP}\,\dot{q}_{\mathrm{ext}} - \dot{q}_c^* \geq 0 \tag{3.74}$$

where $\dot{q}_c^* = 90$ kW/m^2 (see Table 3.8) is the critical heat release rate for sustained burning, then, after removal of the bunsen burner flame when $\dot{q}_{\mathrm{ext}}^* = 0$, burning will only continue if

$$\mathrm{HRR}_0 \geq \dot{q}_c^* = 90\ kW/m^2 \tag{3.75}$$

Eq. (3.74) is a general criterion for sustained, piloted ignition of solids analogous to the fire point equation [3], and Eq. (3.75) is an energy balance criterion for self-sustained burning of plastics. Thus, self-extinguishing behavior in flammability tests after removal of the bunsen burner is expected for HRR_0 less than about 90 kW/m^2. Table 3.12 compares HRR_0 obtained by extrapolation from forced flaming combustion (see Fig. 3.16), measured for self-sustaining combustion under ambient conditions [128], and calculated from the flame heat flux and heat loss measurements [101]. Table 3.12 shows reasonable agreement between HRR_0 obtained in these different ways for a variety of common plastics.

Table 3.13 lists ranked values for HRR_0 of thermoplastics, thermosets, and elastomers obtained from standardized fire calorimetry tests as the heat release rate intercept at zero external heat flux. Included in Table 3.13 are fire retardant (-FR) and glass reinforced (-G) versions of these materials along with a generic UL 94 rating for all of the materials. It is seen that unsteady burning or self-extinguishing behavior in the UL 94 test (V rating) is observed when HRR_0 falls below about 90 kW/m^2, in general agreement with the critical heat release rate at incipient burning (ignition/extinction) deduced from Table 3.8. Toward the bottom of Table 3.13, the HRR_0 assume negative values because halogen-containing/flame-retarded (FR) plastics burn with a low flame heat flux and heat-resistant/thermally stable polymers have large surface heat losses. In either case, the term $\dot{q}_{\mathrm{flame}} - \dot{q}_{\mathrm{loss}}$ in HRR_0 could (and apparently does) assume negative values as per Eq. (3.70).

TABLE 3.12 Intrinsic Heat Release Rates HRR_0 Obtained by Extrapolation from Forced Flaming Combustion Compared to Direct Measurements [128] and Calculation [101] in Self Sustaining Combustion

	HRR_0, kW/m^2		
Polymer	Extrapolated (Table 13)	Measured	Calculated
PET	424 ± 168	353	—
PS	410 ± 66	—	240
PP	369 ± 79	415	202
ABS	359 ± 66	162	—
EVA	—	254	—
PA12	—	245	—
PA66	240 ± 59	—	—
PMMA	217 ± 47	180	240
PA6	187 ± 55	150	—
PE	145 ± 93	75–180	126
POM	162 ± 30	—	148
PC	89 ± 32	5	−200
PEN	57 ± 13	15	—
PF	—	—	16

TABLE 3.13 Intrinsic Heat Release Rate (HRR_0) and Flammability (UL 94 Rating) of Plastics Ranked by HRR_0

Polymer	HRR_0 (kW/m^2)	UL 94 Rating
HIPS	510 ± 77	HB
PP	369 ± 79	HB
PET	424 ± 168	HB
PS	410 ± 66	HB
ABS	359 ± 66	HB
PBT	341 ± 106	HB
UPT	261 ± 105	HB
PC/ABS	259 ± 43	HB
PA66	240 ± 59	HB
PMMA	217 ± 47	HB
PS-FR	205 ± 27	V2
PPO/PS	192 ± 22	HB
PA6	187 ± 55	HB
PC/ABS-FR	178 ± 36	V1
VE	169 ± 44	HB
PESF	168 ± 23	V1
HIPS-FR	164 ± 30	V2
POM	162 ± 30	HB
EP	160 ± 46	HB
PE	145 ± 93	HB
PBT-FR	141 ± 130	V2
ABS-FR	117 ± 33	V2
PVC (flex)	91 ± 19	V2
SIR-M	90 ± 13	V0
PX	88 ±18	V0
PC	89 ± 32	V2
PEN	57 ± 13	V2
ETFE	44 ± 31	V0
PVC (rigid)	9 ± 25	V0
UPT-FR	−31 ± 10	V0
CPVC	−34 ± 9	V0
PE-XL/FR	−38 ± 28	V0
PAI	−64 ± 16	V0
PASF	−83 ± 25	V0
PTFE	−84 ± 9	V0
PESF-G	−89 ± 92	V0
PEEK	−94 ± 20	V0
PEI	−113 ± 19	V0
ECTFE	−127 ± 6	V0
PPS	−147 ± 30	V0
PBI	−150 ± 36	V0
PC-FR	−191 ± 51	V0
TPI	−201 ± 39	V0
PEEK-G	−261 ± 52	V0

The critical heat flux for burning CHF_b is obtained from Eq. (3.68) when $\dot{q}_c = \dot{q}_c^* \approx 90$ kW/m^2 as per Table 3.8

$$CHF_b = \dot{q}_{net}^{crit} = (\dot{q}_{ext} + \dot{q}_{flame} - \dot{q}_{loss}) = \frac{\dot{q}_c^*}{HRP} \approx \frac{90\ kW/m^2}{HRP} \tag{3.76}$$

TABLE 3.14 Critical Heat Fluxes for Ignition (Measured) and Burning (Calculated)

	Critical heat flux, kW/m^2	
Polymer	Ignition	Burning
ABS	9–15	7
CPVC	40	44
ETFE	17–27	15
FEP	38–50	44
PA6	15–20	5
PA66	15–21	5
PAI	40–50	22
PBI	≈60	22
PBT	20	6
PC	15–20	10
PE	15	4
PEEK	30–40	15
PEI	25–40	15
PEN	24	18
PESU	19–30	22
PET	10–19	7
PMMA	6–23	6
POM	13	15
PP	15	4
PPS	35–38	22
PPSU	32–35	22
PS	6–13	5
PTFE	43–50	44
PVC (rigid)	15–28	29
PVDF	30–50	44
SBR	10–15	5
TPI	36–50	18

Table 3.14 compares critical heat fluxes for ignition (CHF) in Table 3.9 to the critical heat flux for sustained burning CHF_b calculated from Eq. (3.76) using the reported HRP for each plastic (Table 3.11). Table 3.14 shows that CHF_b is about 10 kW/m^2 less than CHF on average, but the trend is similar.

DEFINITION OF TERMS

α = thermal diffusivity ($\kappa/\rho c$)

A = global frequency factor for pyrolysis (s^{-1})

A_g = frequency factor for gas generation (s^{-1})

A_c = frequency factor for char formation (s^{-1})

b = sample thickness (m)

β = constant heating rate (K/s)

c_1, c_2 = constants of integration (K)

CHF	=	critical heat flux for piloted ignition (kW/m^2)
CHF_b	=	critical heat flux to sustain burning (kW/m^2)
χ	=	gas phase combustion efficiency (dimensionless)
c	=	heat capacity (J/g·K)
e	=	the natural number 2.718 . . .
ε	=	surface emissivity of radiant energy (dimensionless)
E_a	=	global activation energy for pyrolysis (J/mol)
E_g	=	activation energy for gas formation (J/mol)
E_c	=	activation energy for char formation (J/mol)
EHOC	=	heat of combustion
h	=	average surface convective heat transfer coefficient (W/m^2·K)
h_c^o	=	net heat of complete combustion of pyrolysis gases (J/kg)
$h_{c,p}^o$	=	net heat of complete combustion of solid polymer (J/kg)
h_g	=	heat of gasification per unit mass of polymer (J/kg)
η_c	=	heat release capacity (J/g·K)
HRP	=	heat release parameter, $\chi h_c^o/L_g$ (dimensionless)
HRR_0	=	heat release rate in unforced flaming combustion (kW/m^2)
I^*	=	reactive intermediate for pyrolysis
k_p	=	global Arrhenius rate constant for pyrolysis (s^{-1})
k_g	=	Arrhenius rate constant for gas generation (s^{-1})
k_c	=	Arrhenius rate constant for char formation (s^{-1})
k_i	=	Arrhenius rate constant for initiation of bond breaking (s^{-1})
k_r	=	Arrhenius rate constant for bond recombination (s^{-1})
κ	=	thermal conductivity (W/m·K)
L_g	=	heat of gasification per unit mass of volatile fuel (kJ/g)
m	=	instantaneous sample mass (kg)
m_o	=	initial sample mass (kg)
$\dot{m}_{max}$	=	peak mass loss rate (kg/s)
μ	=	char yield or pyrolysis residue of polymer at 850°C (g/g)
M_g	=	molecular weight of gaseous decomposition species (g/mol)
M	=	monomer molecular weight (g/mol)
$\dot{Q}_c$	=	kinetic heat release rate (W/kg)
$\dot{q}_c$	=	heat release rate (HRR) in flaming combustion (kW/m^2)
$\dot{q}_{cr}$	=	critical heat flux (CHF) for piloted ignition (kW/m^2)

$\dot{q}_{ext}$ = external heat flux in a fire or test (kW/m^2)

$\dot{q}_{net}$ = net heat flux to the surface of a burning sample (W/m^2)

$\dot{q}_{flame}$ = flame heat flux (W/m^2)

$\dot{q}_{loss}$ = heat losses per unit area of surface (kW/m^2)

ρ = density (kg/m^3)

r = mass loss rate exponent $(1 + 2RT_p/E_a)^{-1}$ (dimensionless)

R = ideal gas constant (= 8.314 J/mol·K)

σ = Boltzmann radiation constant = 5.7×10^{-8} W/m^2·K^4

S = surface area (m^2)

t = time (s)

t_{ign} = time to piloted ignition at a constant heat flux (s)

T_p = temperature at peak pyrolysis rate at constant heating rate

T_s = sample or surface temperature

T_o = ambient (room) temperature (298 K)

T_d = onset temperature of thermal degradation

T_{ign} = surface temperature at piloted ignition

TRP = thermal response parameter (kW·s$^{1/2}$/m^2) or (kW·s$^{1/2}$·m^{-2})

v = surface recession velocity/burning rate (m/s)

V = volume (m^3)

Y_c = temperature-dependent char yield (dimensionless)

REFERENCES

1. Hilado, C.J., *Flammability Handbook for Plastics,* 5th edition, Technomic Publishing Co., Lancaster, PA, 1998.
2. *The SFPE Handbook of Fire Protection Engineering,* 3rd edition, Society of Fire Protection Engineers, Boston, MA, 2002.
3. Drysdale, D., *An Introduction to Fire Dynamics,* 2nd edition, John Wiley & Sons, New York, 1998.
4. Quintiere, J.G., *Principles of Fire Behavior,* Del Mar Publishers, Albany, NY, 1998.
5. Cullis, C.F., and Hirschler, M.M., *The Combustion of Organic Polymers,* Clarendon Press, Oxford, UK, 1981.
6. Aseeva, R.M., and Zaikov, G.E, *Combustion of Polymer Materials,* Hanser, New York, 1985.
7. Nelson, G.L., ed., *Fire and Polymers: Hazards Identification and Prevention,* ACS Symposium Series 425, American Chemical Society, Washington, DC, 1990.
8. Babrauskas, V., and Grayson, S.J., eds., *Heat Release in Fires,* Elsevier Applied Science, New York, 1992.
9. Le Bras, M., Camino, G., Bourbigot, S., and Delobel, R., *Fire Retardancy of Polymers: The Use of Intumescence,* The Royal Society of Chemistry, Cambridge, UK, 1998.
10. Horrocks, A.R., and Price, D., eds., *Fire Retardant Materials,* Woodhead Publishing, Ltd., Cambridge, UK, 2001.
11. Friedman, R., *Principles of Fire Protection Chemistry and Physics,* National Fire Protection Association, Quincy, MA, 1998.

12. Troitzsch, J., *International Plastics Flammability Handbook,* 2nd edition, Carl Hanser, Munich, Germany, 1990.
13. Grand, A.F, Wilkie, and C.A., eds., *Fire Retardancy of Polymeric Materials,* Marcel Dekker, Inc., NY, 2000.
14. Landrock, A.H., *Handbook of Plastics Flammability and Combustion Toxicology,* Noyes Publications, Park Ridge, NJ, 1983.
15. Fire, F.L., *Combustibility of Plastics,* Van Nostrand Reinhold, New York, 1991.
16. Pal, G., and Macskasy, H., *Plastics: Their Behavior in Fires,* Elsevier, New York, 1991.
17. Nelson, G.L., ed., *Fire and Polymers II: Materials and Tests for Hazard Prevention,* ACS Symposium Series 599, American Chemical Society, Washington, DC, 1995.
18. Glassman, I., *Combustion,* 3rd edition, Academic Press, New York, 1996.
19. Turns., S.R., *An Introduction to Combustion—Concepts and Applications,* McGraw-Hill, New York, 1996.
20. Strehlow, R.A., *Combustion Fundamentals,* McGraw-Hill, New York, 1984.
21. *Flammability of Plastic Materials,* UL 94 Section 2 (Horizontal: HB) and Section 3 (Vertical: V-0/1/2), Underwriters Laboratories Inc., Northbrook, IL, 1991.
22. *Plastics 1980: A Desktop Data Bank,* The International Plastics Selector, Cordura Publications, Inc., La Jolla, CA, 1979.
23. Kennedy, G.F., *Engineering Properties and Applications of Plastics,* John Wiley & Sons, New York, 1957.
24. Gent, A.N., ed., *Engineering with Rubber,* Hanser Publishers, Munich, Germany, 1992.
25. Hartwig, G., *Polymer Properties at Room and Cryogenic Temperatures,* Plenum Press, New York, 1994.
26. Goldsmith, A., Waterman, T.E., and Hirschorn, H.J., eds., *Handbook of Thermophysical Properties of Solid Materials,* MacMillan, New York, 1961.
27. Mark, J.E., ed., *Physical Properties of Polymers Handbook,* American Institute of Physics, Woodbury, NY, 1996.
28. *Modern Plastics Encyclopedia,* McGraw-Hill, New York, 1988.
29. Bicerano, J., *Prediction of Polymer Properties,* 2nd edition, Marcel Dekker, Inc., New York, 1996.
30. Van Krevelen, D.W., *Properties of Polymers,* 3rd edition, Elsevier Scientific, New York, 1990.
31. Thompson, E.V., *Thermal Properties, in Encyclopedia of Polymer Science and Engineering,* Vol. 16, John Wiley & Sons, New York, 1989, pp. 711–747.
32. Touloukian, Y.S., ed., *Thermophysical Properties of High Temperature Solid Materials,* Vol. 6: Intermetallics, Cermets, Polymers and Composite Systems, Part II, MacMillan, New York, 1967.
33. Touloukian, Y.S., Powell, R.W., Ho, C.Y., and Nicolaou, M.C., eds., "Thermal Diffusivity," in *Thermophysical Properties of Matter,* Vol. 10, Plenum Press, New York, 1973.
34. Kishore, K., and Pai Verneker, V.R., "Correlation Between Heats of Depolymerization and Activation Energies in the Degradation of Polymers," *Journal of Polymer Science, Polymer Letters,* 14: 7761–7765, 1976.
35. Brandrup, J., and Immergut, E.H., eds., *Polymer Handbook,* 3rd edition, John Wiley & Sons, New York, 1989.
36. *Engineered Materials Handbook,* Vol. 2, Engineering Plastics. ASM International, Metals Park, OH, 1988.
37. *Plastics Digest,* 17(1): 773–889, 1996.
38. *Engineered Materials Handbook,* Vol. 2, Engineering Plastics, ASM International, Metals Park, OH, 1988.
39. Bhowmik, A.K., and Stephens, H.L., *Handbook of Elastomers,* 2nd edition, Marcel Dekker, Inc. New York, 2001.
40. Thornton, W., "The Role of Oxygen to the Heat of Combustion of Organic Compounds," *Philosophical Magazine and Journal of Science,* 33: 196–205, 1917.
41. Hugget, C., "Estimation of Rate of Heat Release by Means of Oxygen Consumption Measurements," *Fire and Materials,* 4(2): 61–65, 1980.
42. Janssens, M., and Parker, W.J., "Oxygen Consumption Calorimetry," in Babrauskas, V., Grayson, S.J., eds., *Heat Release in Fires,* Elsevier Applied Science, London, 1992, pp. 31–59.
43. Babrauskas, V., "Heat of Combustion and Potential Heat," in Babrauskas, and V., Grayson, S.J., eds., *Heat Release in Fires,* Elsevier Applied Science, London, 1992, pp. 207–223.

44. Walters, R.N., Hackett, S.M., and Lyon, R.E., "Heats of Combustion of High Temperature Polymers," *Fire and Materials,* 24(5): 245–252, 2000.
45. Lowrie, R., *Heat of Combustion and Oxygen Compatibility, Flammability and Sensitivity of Materials in Oxygen-Enriched Atmospheres,* ASTM STP 812, B. Werley, ed., American Society for Testing of Materials, Philadelphia, PA, 1983.
46. Van Krevelen, D.W., "Some Basic Aspects of Flame Resistance of Polymeric Materials," *Polymer,* 16: 615–620, 1975.
47. Wolfs, P.M., Van Krevelen, D.W., and Waterman, H.I., *Brennstoff Chemie,* 40: 155–189, 1959.
48. Montaudo, G., and Puglisi, C., "Thermal Degradation Mechanisms in Condensation Polymers," in Grassie, N., ed., *Developments in Polymer Degradation,* Vol. 7, Elsevier Applied Science, New York, 1977, pp. 35–80.
49. Grassie, N., and Scotney, A., "Activation Energies for the Thermal Degradation of Polymers," in Brandrup, J., Immergut, E.H., eds., *Polymer Handbook,* 2nd edition, Wiley Interscience, New York, 1975, pp. 467–47.
50. Lyon, R.E., "Heat Release Kinetics," *Fire and Materials,* 24(4): 179–186, 2000.
51. Grassie, N., "Products of Thermal Degradation of Polymers," in Brandrup, J., and Immergut, E.H., eds., *Polymer Handbook,* 3rd edition, Wiley Interscience, New York, 1989, pp. 365–397.
52. Lyon, R.E., "Solid State Thermochemistry of Flaming Combustion," in Grand, A.F., and Wilkie, C.A., eds., *Fire Retardancy of Polymeric Materials,* Marcel Dekker, Inc., New York, 2000, pp. 391–44745.
53. Broido, A., and Nelson, M.A., "Char Yield on Pyrolysis of Cellulose," *Combustion and Flame,* 24: 263–268, 1975.
54. DiBlasi, C., "Analysis of Convection and Secondary Reaction Effects Within Porous Solid Fuels Undergoing Pyrolysis," *Combustion Science and Technology,* 90: 315–340, 1993.
55. Shafizadeh, F., "Pyrolysis and Combustion of Cellulosic Materials," *Advances in Carbohydrate Chemistry,* 23: 419–425, 1968.
56. Milosavljevic, I., and Suuberg, E.M., "Cellulose Thermal Decompositon Kinetics: Global Mass Loss Kinetics," *Industrial and Engineering Chemistry Research,* 34(4): 1081–1091, 1995.
57. Lewellen, P.C., Peters, W.A., and Howard, J.B., "Cellulose Pyrolysis Kinetics and Char Formation Mechanism," *Proceedings of the 16th International Symposium on Combustion,* The Combustion Institute, 1976, pp. 1471–1480.
58. Nam, J.D., and Seferis. J.C., "Generalized Composite Degradation Kinetics for Polymeric Systems Under Isothermal and Nonisothermal Conditions," *Journal of Polymer Science: Part B, Polymer Physics,* 30: 455–463, 1992.
59. Day, M., Cooney, J.D., and Wiles. D.M., "A Kinetic Study of the Thermal Decomposition of Poly(Aryl-Ether-Ether-Ketone) in Nitrogen," *Polymer Engineering and Science,* 29: 19–22, 1989.
60. Friedman, H.L., "Kinetics of Thermal Degradation of Char Forming Plastics from Thermogravimetry: Application to a Phenolic Plastic," *Journal of Polymer Science: Part C,* 6: 183–195, 1962.
61. Wall, L.A., "Pyrolysis of Polymers," in *Flammability of Solid Plastics,* Vol. 7, Fire and Flammability Series, Technomic Publishers, Westport, CT, 1974, pp. 323–352.
62. Lyon, R.E., "Pyrolysis Kinetics of Char Forming Polymers," *Polymer Degradation and Stability,* 61: 201–210, 1998.
63. Stags, J.E.J., "Modeling Thermal Degradation of Polymers Using Single-Step First-Order Kinetics," *Fire Safety Journal,* 32: 17–34, 1999.
64. Lyon, R.E., "An Integral Method of Nonisothermal Kinetic Analysis," *Thermochimica Acta,* 297: 117–124, 1997.
65. Gandhi, S., Walters, R.N., and Lyon, R.E., "Cone Calorimeter Study of Cyanate Esters for Aircraft Applications," 27th International Conference on Fire Safety, San Francisco International Airport, CA, Jan. 11–15, 1999.
66. Gandhi, S., and Lyon, R.E., "Ignition and Heat Release Parameters of Engineering Polymers," *PMSE Preprints,* 83, ACS National Meeting, Washington, DC, August 2000.
67. FAA unpublished results.
68. Drysdale, D.D., and Thomson, H.E., "The Ignitability of Flame Retarded Plastics," in Takashi, T., ed., *Proceedings of the 4th International Symposium on Fire Safety Science,* IAFSS, 1994, pp. 195–204.

69. Grand, A.F., "The Use of the Cone Calorimeter to Assess the Effectiveness of Fire Retardant Polymers Under Simulated Real Fire Test Conditions," *Interflam 96,* Interscience Communications, Ltd, London, 1996, pp. 143–152.

70. Tewarson, A., Abu-Isa, I., Cummings, D.R., and LaDue, D.E., "Characterization of the Ignition Behavior of Polymers Commonly Used in the Automotive Industry," *Proceedings 6th International Symposium on Fire Safety Science,* International Association for Fire Safety Science, 2000, pp. 991–1002.

71. Tewarson, A., "Generation of Heat and Chemical Compounds in Fires," in *SFPE Handbook of Fire Protection Engineering,* 3rd edition, Society of Fire Protection Engineers, Boston, MA, Section 3, 2002, pp. 82–161.

72. Lyon, R.E., "Heat Release Capacity: A Molecular Level Fire Response Parameter," 7th International Symposium on Fire Safety Science, Worcester Polytechnic Institute, Worcester, MA, June 16–21, 2002.

73. Lyon, R.E., and Walters, R.N., "A Microscale Combustion Calorimeter," Final Report DOT/FAA/AR-01/117; "Pyrolysis-Combustion Flow Calorimetry," *Journal of Analytical and Applied Pyrolysis* (in press).

74. Walters, R.N., and Lyon, R.E., "Calculating Polymer Flammability from Molar Group Contributions," Final Report DOT/FAA/AR-01/31, September 2001.

75. Parker, W., and Filipczak, R., "Modeling the Heat Release Rate of Aircraft Cabin Panels in the Cone and OSU Calorimeters," *Fire and Materials,* 19: 55–59, 1995.

76. Zhou, Y.Y., Walther, D.C., and Fernandez-Pello, A.C., *Combustion and Flame,* 131: 147–158, 2002.

77. Wichman, I.S., and Atreya, A., "A Simplified Model for the Pyrolysis of Charring Materials," *Combustion and Flame,* 68: 231–247, 1987.

78. Bucsi, A., and Rychly, J., "A Theoretical Approach to Understanding the Connection Between Ignitability and Flammability Parameters of Organic Polymers," *Polymer Degradation and Stability,* 38: 33–40, 1992.

79. Moghtaderi, B., Novozhilov, V., Fletcher, D., and Kent, J.H., "An Integral Model for the Transient Pyrolysis of Solid Materials," *Fire and Materials,* 21: 7–16, 1997.

80. Quintiere, J.G., and Iqbal, N., "An Approximate Integral Model for the Burning Rate of a Thermoplastic-Like Material," *Fire and Materials,* 18: 89–98, 1994.

81. Kanury, A.M., "Flaming Ignition of Liquid Fuels," in *SFPE Handbook of Fire Protection Engineering,* 3rd edition, Society of Fire Protection Engineers, Boston, MA, Section 2, 2002, pp. 188–199.

82. Kanury, A.M., "Flaming Ignition of Solid Fuels," in *The SFPE Handbook of Fire Protection Engineering,* 3rd edition, Society of Fire Protection Engineers, Boston, MA, Section 2, 2002, pp. 229–245.

83. Kanury, A.M., *Introduction to Combustion Phenomena,* Gordon and Breach Science Publishers, New York, 1977.

84. Rasbash, J.D., "Theory in the Evaluation of Fire Properties of Combustible Materials," *Proceedings of the 5th International Fire Protection Seminar,* Karlsruhe, September 1976, pp. 113–130.

85. Standard Test Method for Ignition Properties of Plastics, ASTM D 1929, American Society for Testing and Materials, Philadelphia, PA.

86. Standard Test Method for Heat and Visible Smoke Release Rates for Materials and Products Using an Oxygen Consumption Calorimeter, ASTM E 1354, American Society for Testing and Materials, Philadelphia, PA.

87. Standard Test Method for Measurement of Synthetic Polymer Material Flammability Using a Fire Propagation Apparatus, ASTM E 2058, American Society for Testing and Materials, Philadelphia, PA.

88. Tewarson, A., "Experimental Evaluation of Flammability Parameters of Polymeric Materials," in Lewin, M., and Pearce, E.M., eds., *Flame Retardant Polymeric Materials,* Plenum Press, New York, 1982, pp. 97–153.

89. Carslaw, H.S., and Jaeger, J.C., *Conduction of Heat in Solids,* 2nd edition, Clarendon Press, Oxford, UK, 1976, pp. 50–193.

90. Tewarson, A., "Flammability Parameters of Materials: Ignition, Combustion, and Fire Propagation," *Journal of Fire Sciences,* 12(4): 329–356, 1994.

91. Quintiere, J.G., and Harkelroad, M.T., "New Concepts For Measuring Flame Spread Properties," in Harmathy, T.Z., ed., *Fire Safety Science and Engineering, Special Technical Publication 882,* American Society for Testing and Materials, Philadelphia, PA, 1985, pp. 239–267.

92. Babrauskas, V., "The Cone Calorimeter," in Babrauskas, V., and Grayson, S.J., eds., *Heat Release in Fires,* Elsevier Applied Science, London, UK, 1992, Chapter 4, pp. 87–88.

93. Grand, A.F., "Heat Release Calorimetry Evaluations of Fire Retardant Polymer Systems," *Proceedings of the 42nd International SAMPE Symposium,* 42, 1997, pp. 1062–1070.
94. Tewarson, A., and Chin, W., Shuford, R., An Exploratory Study on High Energy Flux (HEF) Calorimeter to Characterize Flammability of Advanced Engineering Polymers, Phase 1—Ignition and Mass Loss Rate, ARL-TR-2102, October 1999.
95. Gandhi, S., Walters, R.N., and Lyon, R.E., "Fire Performance of Advanced Engineering Thermoplastics," *Proceedings of the 6th International Conference on Fire and Materials,* San Antonio, TX, Feb. 22–23, 1999.
96. Effectiveness of Fire Retardant Chemicals at Elevated Temperatures, Phase I SBIR Final Report, U.S. DOT Contract Number DTRS-57-94C-00172, Omega Point Laboratories, May 1995.
97. Innovative Fire Retardant Polymeric Systems, Phase II SBIR Final Report, U.S. DOT Contract Number DTRS-57-96-00011, Omega Point Laboratories, February 2000.
98. Hirschler, M.M., "Heat Release from Plastic Materials," in Babrauskas, V., and Grayson, S., eds., *Heat Release in Fires,* Elsevier Applied Science, New York, pp. 207–232, 1992.
99. Scudamore, M.J., Briggs, P.J., and Prager, F.H., "Cone Calorimetry—A Review of Tests Carried Out on Plastics for the Association of Plastic Manufacturers in Europe," *Fire and Materials,* 15: 65–84, 1991.
100. Hallman, J.R., *Ignition Characteristics of Plastics and Rubber,* Ph.D. dissertation, University of Oklahoma, Norman, OK, 1971.
101. Tewarson, A., and Pion, R.F., "Flammability of Plastics: I. Burning Intensity," *Combustion and Flame,* 26: 85–103, 1976.
102. Tewarson, A., "Heat Release Rates from Burning Plastics," *Journal of Fire & Flammability,* 8: 115–130, 1977.
103. Tewarson, A., "Flammability Evaluation of Clean Room Polymeric Materials for the Semiconductor Industry," *Fire and Materials,* 25: 31–42, 2001.
104. Tewarson, A., Abu-Isa, I.A., Cummings, D.R., and LaDue, D.E., "Characterization of the Ignition Behavior of Polymers Commonly Used in the Automotive Industry," *Proceedings of the 6th International Symposium on Fire Safety Science,* Poitiers, France, 1999, pp. 991–1002.
105. Gandhi, S., Walters, R.N., and Lyon, R.E., "Heat Release Rates of Engineering Polymers," *Proceedings of the 6th International Conference on Fire and Materials,* San Antonio, TX, February 1999.
106. Buch, R.R., "Rates of Heat Release and Related Fire Parameters for Silicones," *Fire Safety Journal,* 17: 1–12, 1991.
107. Hsieh, F.Y, Motto, S.E., Hirsch, D.B., and Beeson, H.D., "Flammability Testing Using a Controlled Atmosphere Cone Calorimeter," presented at the Eighth International Conference on Fire Safety, Milbrae, CA, 1993.
108. Koo, J., Venumbaka, S., Cassidy, P., Fitch, J., Grand, A., and Burdick, J., "Evaluation of Thermally Resistant Polymers Using Cone Calorimetry," *Proceedings of the 5th International Conference on Fire and Materials,* San Antonio, TX, February 23–24, 1998, pp. 183–193.
109. Staggs, J.E.J., "Discussion of Modeling Idealized Ablative Materials with Particular Reference to Fire Testing," *Fire Safety Journal,* 28: 47–66, 1997.
110. Whiteley, R.H., Elliot, P.J., and Staggs, J.E.J., "Steady-State Analysis of Cone Calorimeter Data," *Flame Retardants '96,* Interscience Communications, Ltd., London, pp. 71–78, 1996.
111. Lyon, R.E., "Ignition Resistance of Plastics," *13th Annual BCC Conference on Flame Retardancy of Polymeric Materials,* Stamford, CT, June 3–5, 2002.
112. Tewarson, A., Lee, J.H., and Pion, R.F., "The Influence of Oxygen Concentration on Fuel Parameters for Fire Modeling," *Proceedings of the Eighteenth Symposium (International) on Combustion,* The Combustion Institute, Pittsburgh, PA, 1981, pp. 563–570.
113. Babrauskas, V., and Peacock, R.D., "Heat Release Rate: The Single Most Important Variable in Fire Hazard," *Fire Safety Journal,* 18: 255–272, 1992.
114. Calculation based on U.S. Department of Commerce data for dollar value of flame retardants sold in U.S. and Society of Plastics Industry database on U.S. Plastics sales by use (NAICS) category assuming annual worldwide consumption of FR plastics is three times that of U.S.
115. Standard Test Method for Measuring the Minimum Oxygen Concentration to Support Candle-Like Combustion of Plastics (Oxygen Index), ASTM D 2863, American Society for Testing of Materials, Philadelphia, PA.

116. Gandhi, P.D., "Comparison of Cone Calorimeter Results with UL94 Classification for Some Plastics," presented at the 5th Annual BCC Conference on Flame Retardancy, Stamford, CT, May 24–26, 1994.

117. Bundy, M., National Institute of Standards and Technology, Gaithersburg, MD, private communication.

118. Hill, R.G., Eklund, T.I., and Sarkos, C.P., Aircraft Interior Panel Test Criteria Derived From Full Scale Fire Tests, Federal Aviation Administration Report DOT/FAA/CT-85/23, September 1985.

119. Sarkos, C.P., Filipczak, R.A.. and Abramowitz, A., A Preliminary Evaluation of an Improved Flammability Test Method for Aircraft Materials, Federal Aviation Administration Report DOT/FAA/CT-84/22, December 1984.

120. Babrauskas, V., Fire Hazard Comparison of Fire-Retarded and Non Fire-Retarded Products, NBS Special Publication, SP749, National Institute of Standards and Technology, USA, 1988.

121. Simonson, M., and DePoortere, M., "The Fire Safety of TV Set Enclosure Material," presented at Fire Retardant Polymers, 7th European Symposium, Lille, France, 1999.

122. Bailey, R., and Blair, G., "Small Scale Laboratory Flammability Testing and Real Automotive Interior Fires," presented at Fire Retardant Chemical Association Meeting, Philadelphia, PA, October 14–16, 2001.

123. Grayson, S., "Fire Performance of Plastics in Car Interiors," *Proceedings of Flame Retardants 2002,* London, UK, February 2002.

124. Le Tallec, Y., Sainratm, A., and Strugeon, A., "The Firestarr Project–Fire Protection of Railway Vehicles," *Proceedings Fire & Materials 2001, 7th International Conference and Exhibition,* San Francisco, CA, January 22–24, 2001.

125. Babrauskas, V., "The Effects of FR Agents on Polymer Performance," in Babrauskas, V., and Grayson, S., eds., *Heat Release In Fires,* Elsevier Applied Science, New York, 1992, pp. 423–446.

126. Burgess, M.J., and Wheeler, R.V., *Journal of the Chemical Society,* 99: 2013, 1911.

127. Lyon, R.E., "Fire and Flammability," Fire & Materials Conference, San Francisco, CA, January 2003.